



Uncertainty quantification and global sensitivity analysis for progressive failure of fiber-reinforced composites

Mishal Thapa¹ · Achyut Paudel¹ · Sameer B. Mulani¹ · Robert W. Walters²

Received: 12 March 2020 / Revised: 31 May 2020 / Accepted: 13 July 2020 / Published online: 26 August 2020
© Springer-Verlag GmbH Germany, part of Springer Nature 2020

Abstract

In this paper, a framework for the stochastic progressive failure analysis (PFA) of fiber-reinforced composites is presented. The nonlinear responses of composite structures are hugely influenced by the randomness in material properties of plies, thereby yielding significantly different responses compared with that with deterministic simulations. Moreover, performing PFA using finite element analysis (FEA) is a computationally intensive process that becomes unaffordable while performing uncertainty analysis that requires numerous FEA runs. So, to alleviate this computational cost while maintaining an acceptable accuracy, an efficient technique called polynomial chaos expansion (PCE) was implemented. Another advantage of PCE is that it allows performing global sensitivity analysis (GSA) to estimate the influence of the random inputs on the stochastic responses as a post-processing step without any additional cost. The effects of randomness in material properties on the first ply failure load and ultimate failure responses of a composite laminate were compared with the framework using PCE as well as 5000 LHS simulations and the results underlined the cost-effectiveness as well as the high accuracy of PCE. Moreover, the GSA successfully identified the influential random material properties that correlated well with the failure modes. Thus, the presented approach and the results of this study will be instrumental in understanding the failure as well as improving the design of composite structures.

Keywords Fiber-reinforced composites · Progressive failure analysis · Uncertainty quantification · Global sensitivity analysis · Puck failure criterion

1 Introduction

The tremendous growth in applications of composite structures in several disciplines such as aerospace, automotive,

marine, and sports, can be attributed to its superior characteristics such as high stiffness/strength to weight ratio, tailorability, durability, and manufacturability (Kanouté et al. 2009). The application of the composite structures is expected to grow further in the near future due to an improvement in the understanding of the behavior of composites and the developments of state of the art manufacturing technologies. However, we are still unable to fully comprehend the complex failure mechanisms and damage mechanics of composite structures due to its non-homogeneous and orthotropic nature which results in the occurrence of a failure in composites in a progressive manner. This necessitates the development of appropriate computational methods that can incorporate the intricacies of the actual failure behavior so that the number of expensive experimental tests can be somehow alleviated with the development of robust (reliable) numerical models in the early stage of composite structures design. Furthermore, since the responses of composites are hugely influenced by the presence of various uncertainties during design, fabrication/manufacturing, transport, and environmental as well

Responsible Editor: Helder C. Rodrigues

✉ Mishal Thapa
mthapa@crimson.ua.edu

Achyut Paudel
apaudel@crimson.ua.edu

Sameer B. Mulani
sbmulani@eng.ua.edu

Robert W. Walters
rwalters@vt.edu

¹ The University of Alabama, Tuscaloosa, AL 35487, USA

² Virginia Polytechnic Institute and State University, Blacksburg, VA 24061, USA

as operating conditions, one should account the effects of these uncertainties on the responses by performing uncertainty quantification (UQ) and also estimate its influence on the variation of responses by performing global sensitivity analysis (GSA) (Thapa et al. 2019c). Carrying out UQ and GSA improves the performance and reliability of composite structures; however, the main bottleneck in utilizing it for the PFA of composites is that it is a computationally expensive process even with the existing state of the art computational technologies, which becomes a daunting task while considering complex composite structures. Therefore, it is paramount to develop a computationally efficient framework for stochastic PFA of composites to aid the designers and engineers.

Failure in laminated composite structures can be classified as intralaminar and interlaminar, which results in significant degradation of the performance of composites. The intralaminar failure includes failure modes such as breaking of fibers, matrix cracking, and fiber-matrix debonding, whereas the interlaminar failure consists of delamination. Interestingly, both of these failures occur in a progressive manner and mostly on a ply-by-ply basis (Murugesan and Rajamohan 2017; Tay et al. 2008; Sleight 1999; Garnich and Akula 2009) because of several factors such as the different amount of loads shared by the plies, the different load-carrying capacity of the plies depending on the ply orientation, stacking sequence, the thickness of the plies, and location of the plies from the reference mid-plane. In reality, the composite structures are capable of withstanding loads beyond the first ply failure load. After the first occurrence of a failure of a ply, the load is shared among the remaining plies. The failure of next ply occurs upon increasing the load, and the process of sharing the loads among the remaining undamaged plies is repeated until all of the plies fail, which indicates the structure is no longer able to sustain the additional load. The load at which the failure of the first ply occurs is known as the first ply failure (FPF) load, and the load at which the failure of the last ply occurs is known as the last ply failure (LPF) load. Similarly, the peak or ultimate load, after which a decreasing trend in load vs. displacement is observed, can also be used to estimate catastrophic/ultimate failure in some cases. So, since the composite structures are capable of carrying loads beyond the first ply failure, it is necessary to perform nonlinear analysis and also estimate the ultimate and the last ply failure loads to exploit the benefits of composites fully.

To estimate the ultimate and the last ply failure loads beyond FPF, the progressive failure analysis (PFA) approach should be utilized, and two of the main ingredients for PFA of composites are the failure criteria and material property degradation models (MPDM). The failure criteria are required to detect the occurrence of a failure in the plies, whereas the MPDM is required to account for the damage

of the failed plies and reduce the material property/stiffness accordingly. There are numerous failure criteria available all of which can be classified as either mode-independent or mode-dependent. The mode-independent failure criteria do not identify the mode of damage, whereas the mode-dependent failure criteria can identify the modes of failure. Some of the mode-independent failure criteria are maximum stress/strain, Tsai-Hill, Tsai-Wu, and Hoffman criterion whereas some of the mode-dependent failure criteria are the Hashin-Rotem, Hashin, and Puck criterion (Hinton et al. 2002; 2004; Daniel 2007; Icardi et al. 2007). The choice of failure criterion affects the failure prediction of composite structures, and a proper analysis should be carried out before deciding on a particular failure criterion. In addition to the failure criterion, the degradation models used to account for the progression of damage also affect the non-linear response of a composite. Two of the widely used degradation models are the ply-discount method or the immediate degradation method and the gradual degradation method. The ply-discount method neglects the contribution of failed plies in carrying the loads, whereas the gradual degradation method accounts for the contribution of failed plies until the degradation factor reaches a minimal value. Hence, a proper selection of failure criterion and MPDM should be made during the PFA of composites. The number of studies devoted to PFA of composites using a deterministic approach is innumerable and some of the selected studies are provided in Sun et al. (2001), Pal and Ray (2002), Pal and Bhattacharyya (2007), Lopes et al. (2007), Liu and Zheng (2008), Chen et al. (2014), Ambur et al. (2004), McCartney (2005), Günel and Kayran (2013), Lee et al. (2015), Romanowicz (2010), Chang and Chang (1987), Chang et al. (1988), and Reddy et al. (1995).

As aforementioned, the responses of composite structures are hugely affected by the presence of uncertainties across various scales, such as the variability of constituents (fiber and matrix) properties in micro-scale, the variability in thickness and orientations of the plies in meso-scale, and the loads and boundary conditions in macro-scale. Traditionally, safety factors and knockdown factors are used to account for the influence of uncertainties, which most of the time leads to a conservative design with a substantial increase in weight and make the massive benefits offered by composite unexploitable. Also, sometimes, these factors are not sufficient and lead to the catastrophic failure of composites. Therefore, an alternative to the safety factor approach is the application of a probabilistic approach for UQ while designing composite structures. And, some of the traditional approaches to this end are Monte Carlo simulation (MCS) (Cruz and Patera 1995; Sakata et al. 2008a), perturbation methods (Sakata et al. 2008b; Zhou et al. 2016; Kamiński and Kleiber 2000), stochastic finite

element methods (Kleiber and Hien 1992; Liu et al. 1986), and spectral methods (Ghanem and Spanos 1990). Among these techniques, the spectral approach known as *polynomial chaos expansion (PCE) or simply PC* (Wiener 1938; Choi et al. 2006; Hosder et al. 2006; Hosder et al. 2010; Thapa et al. 2018a; 2018b; 2019c; 2020) remains one of the best options for UQ of PFA of composites because of its mean-square convergence property which is computationally efficient and provides high accuracy. Also, it can handle random inputs with a high variation compared with other approaches. Some of the studies related to forward uncertainty propagation for composite structures are provided in Shaw et al. (2010); Zhou et al. (2016); Sepahvand (2016); Dey et al. (2015, 2017); Thapa et al. (2018a), (2019b), (2020) most of which are focused on linear-static, buckling, and free vibration problems. Surprisingly, there are only a handful of studies related to stochastic PFA and one of the stochastic studies that were available in the literature review was the implementation of a perturbation technique for the random progressive failure of composite laminates by Gadade et al. in (2016) for FPF and LPF load estimation using the Puck failure criterion. The lack of studies related to stochastic PFA is due to the huge computational cost associated with non-linearity that increases exponentially when applying the probabilistic approach.

Furthermore, it is also important to identify the influence of each random input parameter on the response of composites such as FPF load, peak load, and LPF load by performing sensitivity analysis (SA). There are two approaches for performing SA—local and global. While the local SA focuses on estimating the local contribution of random variables using gradient estimation at the mean values, the global SA (GSA) considers the whole range of random inputs and provides the variance contribution of the random inputs on the variance of the responses. Furthermore, GSA allows one to decide which random input parameters should be given more attention to control during manufacturing and which random inputs can be considered as deterministic. Due to this reason, GSA has been utilized in this study. One of the best approaches for performing GSA is using variance-based Sobol indices, which provides both the qualitative information (classification of random inputs) and quantitative information (ranking of the importance of random inputs) (Saltelli et al. 2000; Sudret 2008; Crestaux et al. 2009). The Sobol indices are calculated based on the Sobol decomposition of the variance of uncertain responses such as FPF loads and LPF loads in PFA. Usually, the MCS used to be the preferred approach for estimating Sobol indices. In Navaid (2010), GSA using Sobol indices of the parameters in Puck's failure theory for estimation of the failure load of laminated composites were carried out with only 1000 Latin Hypercube Design samples. In Li et al. (2017), the MCS was utilized to

calculate Sobol indices for GSA of load distribution and displacement of multi-bolt composite joints through the spring-based method. Similarly, the effect of randomness in effective material properties (obtained with asymptotic homogenization and stochastic analysis), ply strength, and ply orientation on the strength of a laminate using an analytical approach with 10,000 MCS was studied in Zhi and Tay (2018). In Zhi and Tay (2018), the sensitivity analysis was carried out as a by-product of stochastic analysis by calculating the correlation of input parameters with the outputs. Although the MCS offers simplicity, the number of samples required to estimate the Sobol indices or sensitivity of random inputs with a desirable accuracy is enormous because of its slow convergence. To avoid a huge number of model evaluations as required in MCS, metamodeling-based GSA for elastic properties of composites was studied in Zhu et al. (2018) by using Kriging. The Kriging-based metamodel was then used to obtain high-dimensional model representation (HDMR) of the elastic properties of the composite that were dependent on the fiber, matrix, and interface properties. Once the HDMR was obtained, the Sobol method was used to estimate the first-order and second-order sensitivity indices. Although the suggested methodology was found to yield good results, the construction of HDMR models seems an additional step since the Kriging metamodels can be directly utilized for the estimation of Sobol indices based on the MCS approach. Therefore, while there are numerous studies available on either deterministic PFA or GSA for an analytical approach-based progressive failure of composite structures separately, a finite-element-based stochastic PFA of composite structures has not been carried out before. So, the implementation of PCE-based GSA for responses obtained from FEA-based PFA to provide an in-depth understanding of failure in composites represents the novelty of our research. In our study, the PCE-based GSA has been adopted since the Sobol indices can be calculated as a post-processing step without any additional significant processing time at a low cost with the total number of function evaluations equivalent to that required for PCE construction only.

Therefore, the primary goal of this paper is to present a stochastic framework using non-intrusive PCE to carry out UQ and GSA of the responses obtained from the PFA of fiber-reinforced composites. To this end, the ingredients for performing PFA of composite laminates, such as the theory of composite laminates, failure criterion, and MPDM, are discussed in Section 2, and the details of UQ and GSA with PCE are provided in Section 3. The methodology for the proposed framework is described in Section 4, and the implementation of this framework to several case studies is provided in Section 5. Finally, the conclusions of this paper are drawn in Section 6.

2 Theory for progressive failure analysis of composites

The PFA of composite structures relies on the analysis of ply-level stress state, which can be obtained by using classical laminate plate theory (CLPT) or shear deformation theories. So, the theory for composite laminates using first-order shear deformation theory (FSDT) is provided in the following subsection.

2.1 First-order shear deformation theory for modeling of composite laminates

A brief discussion of the theory involved in the development of a finite-element model of a composite laminate using FSDT is provided here. The detailed discussions of FSDT are provided in Reddy (2003) and Thapa et al. (2019b).

2.1.1 Constitutive equations

Under the consideration of the presence of uncertainties represented using $\vec{\xi}$, the displacement field at any point (x, y, z) and at any time t based on the FSDT can be given as in (1) for a composite laminate, as shown in Fig. 1. In (1), u_0 , v_0 , and w_0 represent the displacement of a point (x, y) in the mid-plane z_0 , whereas ϕ_x and ϕ_y represent the rotation of transverse normal about y -axis and x -axis, respectively. Therefore, the unknowns in generalized displacements in FSDT are u_0 , v_0 , w_0 , ϕ_x , and ϕ_y . Following (1), the dependence of the stresses, strains, and all other responses on the randomness $\vec{\xi}$ in the input parameters has been omitted for brevity.

Likewise, the non-linear strain-displacement relationship using the displacement field in (1) can be given as in (2). The constitutive equation for a k^{th} layer of a laminate with

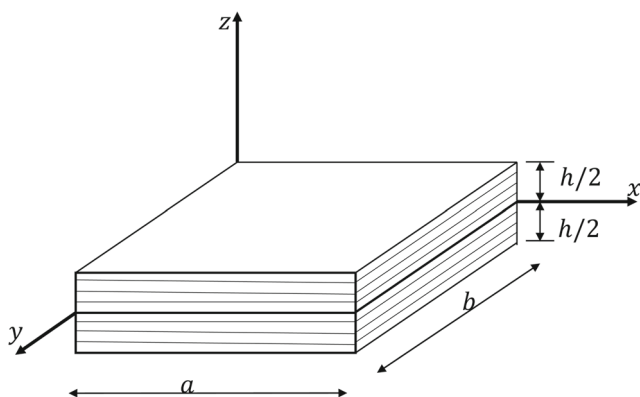


Fig. 1 The geometry and the global coordinate system of a composite laminate

thickness h can be written in the global/laminate coordinate system as in (3). In (3), \bar{Q}_{ij} represents the reduced stiffness components in the global coordinate system that are obtained from the transformation of reduced stiffness components Q_{ij} in (4) by using (5).

$$\begin{aligned} u(x, y, z, t; \vec{\xi}) &= u_0(x, y, t; \vec{\xi}) + z\phi_x(x, y, t; \vec{\xi}) \\ v(x, y, z, t; \vec{\xi}) &= v_0(x, y, t; \vec{\xi}) + z\phi_y(x, y, t; \vec{\xi}) \\ w(x, y, z, t; \vec{\xi}) &= w_0(x, y, t; \vec{\xi}) \end{aligned} \tag{1}$$

$$\begin{aligned} \varepsilon_{xx} &= \frac{\partial u_0}{\partial x} + \frac{1}{2} \left(\frac{\partial w_0}{\partial x} \right)^2 + z \frac{\partial \phi_x}{\partial x} \\ \varepsilon_{yy} &= \frac{\partial v_0}{\partial y} + \frac{1}{2} \left(\frac{\partial w_0}{\partial y} \right)^2 + z \frac{\partial \phi_y}{\partial y} \\ \gamma_{xy} &= \left(\frac{\partial u_0}{\partial y} + \frac{\partial v_0}{\partial x} + \frac{\partial w_0}{\partial x} \frac{\partial w_0}{\partial y} \right) + z \left(\frac{\partial \phi_x}{\partial y} + \frac{\partial \phi_y}{\partial x} \right) \\ \gamma_{xz} &= \frac{\partial w_0}{\partial x} + \phi_x; \quad \gamma_{yz} = \frac{\partial w_0}{\partial y} + \phi_y; \quad \varepsilon_{zz} = 0 \end{aligned} \tag{2}$$

$$\begin{Bmatrix} \sigma_{xx} \\ \sigma_{yy} \\ \sigma_{xy} \\ \sigma_{yz} \\ \sigma_{xz} \end{Bmatrix}^{(k)} = \begin{bmatrix} \bar{Q}_{11} & \bar{Q}_{12} & \bar{Q}_{16} & 0 & 0 \\ \bar{Q}_{21} & \bar{Q}_{22} & \bar{Q}_{26} & 0 & 0 \\ \bar{Q}_{16} & \bar{Q}_{26} & \bar{Q}_{66} & 0 & 0 \\ 0 & 0 & 0 & \bar{Q}_{44} & \bar{Q}_{45} \\ 0 & 0 & 0 & \bar{Q}_{45} & \bar{Q}_{55} \end{bmatrix}^{(k)} \begin{Bmatrix} \varepsilon_{xx} \\ \varepsilon_{yy} \\ \varepsilon_{xy} \\ \varepsilon_{yz} \\ \varepsilon_{xz} \end{Bmatrix} \tag{3}$$

$$\begin{aligned} Q_{11} &= \frac{E_1}{1 - \nu_{12}\nu_{21}}; \quad Q_{12} = \frac{\nu_{12}E_2}{1 - \nu_{12}\nu_{21}}; \quad Q_{22} = \frac{E_2}{1 - \nu_{12}\nu_{21}} \\ Q_{66} &= G_{12}; \quad Q_{44} = G_{23}; \quad Q_{55} = G_{13} \end{aligned} \tag{4}$$

$$\begin{aligned} \bar{Q}_{11} &= Q_{11}.c^4 + 2(Q_{12} + 2Q_{66}).s^2.c^2 + Q_{22}.s^4 \\ \bar{Q}_{12} &= (Q_{11} + Q_{22} - 4Q_{66}).s^2.c^2 + Q_{12}.(s^4 + c^4) \\ \bar{Q}_{22} &= Q_{11}.s^4 + 2(Q_{12} + 2Q_{66}).s^2.c^2 + Q_{22}.c^4 \\ \bar{Q}_{16} &= (Q_{11} - Q_{12} - 2Q_{66}).s.c^3 + (Q_{12} - Q_{22} + 2Q_{66}).s^3.c \\ \bar{Q}_{26} &= (Q_{11} - Q_{12} - 2Q_{66}).s^3.c + (Q_{12} - Q_{22} + 2Q_{66}).s.c^3 \\ \bar{Q}_{66} &= (Q_{11} + Q_{22} - 2Q_{12} - 2Q_{66}).s^2.c^2 + Q_{66}.(s^4 + c^4) \\ \bar{Q}_{44} &= Q_{44}.c^2 + Q_{55}.s^2; \quad \bar{Q}_{45} = (Q_{55} - Q_{44}).c.s \\ \bar{Q}_{55} &= Q_{44}.s^2 + Q_{55}.c^2 \end{aligned} \tag{5}$$

where, $c = \cos(\theta)$ and $s = \sin(\theta)$

Furthermore, the stress resultants of the whole laminate can be obtained using (6) where N , M , and Q represent the in-plane force resultants, moment resultants, and shear force resultants, respectively. The stress resultants can also be expressed in terms of the displacements as in (7) where

A_{ij} , B_{ij} , and D_{ij} are the extensional stiffnesses, bending-extensional stiffnesses, and bending stiffnesses as in (8) whereas κ is the shear correction factor.

$$\begin{aligned} (N_x, N_y, N_{xy}) &= \int_{-h/2}^{h/2} (\sigma_x, \sigma_y, \sigma_{xy}) dz \\ (M_x, M_y, M_{xy}) &= \int_{-h/2}^{h/2} (\sigma_x, \sigma_y, \sigma_{xy}) z dz \\ (Q_x, Q_y) &= \int_{-h/2}^{h/2} (\sigma_{xz}, \sigma_{yz}) dz \end{aligned} \tag{6}$$

$$\begin{aligned} \begin{Bmatrix} N_x \\ N_y \\ N_{xy} \end{Bmatrix} &= \begin{bmatrix} A_{11} & A_{12} & A_{16} \\ A_{21} & A_{22} & A_{26} \\ A_{16} & A_{26} & A_{66} \end{bmatrix} \begin{Bmatrix} \frac{\partial u_0}{\partial x} + \frac{1}{2} \left(\frac{\partial w_0}{\partial x} \right)^2 \\ \frac{\partial v_0}{\partial y} + \frac{1}{2} \left(\frac{\partial w_0}{\partial y} \right)^2 \\ \frac{\partial u_0}{\partial x} + \frac{\partial v_0}{\partial y} + \frac{\partial w_0}{\partial x} \frac{\partial w_0}{\partial y} \end{Bmatrix} \\ &+ \begin{bmatrix} B_{11} & B_{12} & B_{16} \\ B_{21} & B_{22} & B_{26} \\ B_{16} & B_{26} & B_{66} \end{bmatrix} \begin{Bmatrix} \frac{\partial \phi_x}{\partial x} \\ \frac{\partial \phi_y}{\partial y} \\ \frac{\partial \phi_x}{\partial y} + \frac{\partial \phi_y}{\partial x} \end{Bmatrix} \\ \begin{Bmatrix} M_x \\ M_y \\ M_{xy} \end{Bmatrix} &= \begin{bmatrix} B_{11} & B_{12} & B_{16} \\ B_{21} & B_{22} & B_{26} \\ B_{16} & B_{26} & B_{66} \end{bmatrix} \begin{Bmatrix} \frac{\partial u_0}{\partial x} + \frac{1}{2} \left(\frac{\partial w_0}{\partial x} \right)^2 \\ \frac{\partial v_0}{\partial y} + \frac{1}{2} \left(\frac{\partial w_0}{\partial y} \right)^2 \\ \frac{\partial u_0}{\partial x} + \frac{\partial v_0}{\partial y} + \frac{\partial w_0}{\partial x} \frac{\partial w_0}{\partial y} \end{Bmatrix} \\ &+ \begin{bmatrix} D_{11} & D_{12} & D_{16} \\ D_{21} & D_{22} & D_{26} \\ D_{16} & D_{26} & B_{66} \end{bmatrix} \begin{Bmatrix} \frac{\partial \phi_x}{\partial x} \\ \frac{\partial \phi_y}{\partial y} \\ \frac{\partial \phi_x}{\partial y} + \frac{\partial \phi_y}{\partial x} \end{Bmatrix} \\ \begin{Bmatrix} Q_x \\ Q_y \end{Bmatrix} &= \kappa \begin{bmatrix} A_{44} & A_{45} \\ A_{45} & A_{55} \end{bmatrix} \begin{Bmatrix} \frac{\partial w_0}{\partial y} \\ \frac{\partial w_0}{\partial x} \end{Bmatrix} \end{aligned} \tag{7}$$

$$(A_{ij}, B_{ij}, D_{ij}) = \int_{-h/2}^{h/2} \bar{Q}_{ij} (1, z, z^2) dz \tag{8}$$

$$[\mathbf{K}(\{\Delta\})] \{\Delta\} = \{\mathbf{F}\} \tag{9}$$

So, upon the application of the principle of virtual work or Hamilton's principle using force and moment resultants in (7) along with the finite-element formulation for generalized displacement variables, the finite element model of a composite laminate based on FSDT can be obtained. For a non-linear static analysis using FSDT in progressive failure analysis, assembled finite element equations can be written as in (9) which represents a system of nonlinear algebraic equations and must be solved using an iterative method to establish equilibrium (MSC 2007; Reddy 2003; Sleight 1999). In (9), $\{\Delta\}$ represents

the displacement vector, $\{\mathbf{F}\}$ is the applied force vector, and $[\mathbf{K}(\{\Delta\})]$ is a global non-linear stiffness matrix which depends on both the material properties as well as the unknown displacement solution $\{\Delta\}$.

To perform a non-linear analysis, generally the linearized finite element equations for the k^{th} iteration as in (10-11) should be solved for a given load step. Here, $[K_T]^{(k)}$ and $\{r\}^{(k)}$ represent the tangent stiffness matrix and the residual both of which are functions of solution $\{\Delta\}^{(k)}$. The residual represents the difference between the applied load $\{\mathbf{F}\}$ and the internal load $\{\mathbf{R}\}$. Then, based on the tangent stiffness matrix and the residual at the k^{th} iteration, the incremental solution $\{\delta\Delta\}$ can be estimated which is then used to update the solution $\{\Delta\}^{(k+1)}$ in (11). This process is repeated until the convergence of $\{r\}$ and $\{\delta\Delta\}$ to within some tolerance value after which the load is incremented. For this iterative process, different schemes such as Newton-Raphson (which is the default choice in MSC Nastran FEA software), modified Newton-Raphson, and secant method can be used. For more details, please refer to MSC (2007), Reddy (2003), and Sleight (1999):

$$[K_T]^{(k)} \{\delta\Delta\} = \{r\}^{(k)} \tag{10}$$

$$\{\Delta\}^{(k+1)} = \{\Delta\}^{(k)} + \{\delta\Delta\} \tag{11}$$

Since this study is mainly focused on the PFA of composite laminates which involves the geometric non-linearity as well as the degradation of material properties when the failure occurs, the PFA can be carried out along with the above description for non-linear analysis by adopting the following main steps (MSC 2007; Pal and Ray 2002; Sleight 1999; Garnich and Akula 2009):

1. Firstly, for an initial state which is in a static equilibrium, increase the load by a small value.
2. Then, perform a non-linear analysis as in (10-11) until a convergence of the solution is obtained.
3. Based on an equilibrium state of the converged solution, calculate the stresses in the plies of an element at the integration points for a given load level.
4. After obtaining the stresses, apply a failure criterion to examine the failure of plies at the integration points.
5. *If the failure of a ply of an element/elements is detected:*
 - Implement the material property degradation scheme to account for the failed fiber/matrix as given in Section 2.1.2 by reducing the material stiffness accordingly for the failed plies of an element. Then, using the degraded material properties, repeat steps 2-5 at the same load level until no additional ply failure of any elements is detected.

Else if no failure is detected:

- Continue to Step 6.

6. Then, increase the load and repeat steps 2–6 until the final value of the load is attained or ultimate failure is observed.

Note that the PFA can be carried out using the load control or the displacement control. In the case of the load control, the load increment in the above steps for PFA indicates the increase in applied load whereas in the displacement control, the load increment indicates the increase in applied displacement. It is to be noted that both approaches require performing all of the steps 1–6. However, since the load control can cause stability issues near peak load (MSC 2007), the displacement control is used in most of the cases and has been implemented for this study.

Also, note that only intralaminar failure has been considered in this study since the implementation of stochastic interlaminar failure demands a separate investigation that will be included in subsequent research.

2.1.2 Puck failure criterion

There are a lot of failure criteria available for detecting the failure in plies, as mentioned in the literature review. However, based on the World-Wide Failure Exercise (Soden et al. 2004), the Puck criterion was found to be the most accurate and yielded similar results as experiments. Hence, the Puck failure criterion was used in this study.

The Puck failure criterion (Puck and Schürmann 2004) is a mode-dependent failure criterion, which means that it can detect a failure based on five different modes as given in (12–16). This feature allows for the degradation of the respective material/stiffness properties according to the mode of failure. In (12–16), ϵ_1 , ϵ_{1T} , and ϵ_{1C} represent the current strain, strain in tension failure, and strain in compression failure; ν_{f12} and E_{f1} are Poisson’s ratio and Young’s modulus of fiber; $m_{\sigma f}$ is the stress magnification factor for the fibers in material direction 2 (1.1 for carbon fiber and 1.3 for glass fiber (Navaid 2010; Murugesan and Rajamohan 2017)); σ_{11} and σ_{22} are the normal (current) stress in material directions 1 and 2; τ_{21} , γ_{21} , and S_{21} are the shear stress, shear strain, and shear strength; σ_{11D} is the stress value for linear degradation in material coordinate system; Y_T and Y_C are the in-plane tensile and compressive strength perpendicular to fiber direction (transverse direction); and p_{vp}^+ , p_{vp}^- , and p_{vv}^- are the Puck’s parameters depending on the fracture plane angles.

1. Fiber failure in tension

$$\frac{1}{\epsilon_{1T}} \left(\epsilon_1 + \frac{\nu_{f12}}{E_{f1}} m_{\sigma f} \sigma_{22} \right) = 1 \tag{12}$$

2. Fiber failure in compression

$$\frac{1}{\epsilon_{1C}} \left| \epsilon_1 + \frac{\nu_{f12}}{E_{f1}} m_{\sigma f} \sigma_{22} \right| + (10\gamma_{21})^2 = 1 \tag{13}$$

3. Matrix failure in in-plane transverse tension

$$\sqrt{\left(\frac{\tau_{21}}{S_{21}} \right)^2 + \left(1 - p_{vp}^+ \frac{Y_T}{S_{21}} \right)^2 \left(\frac{\sigma_{22}}{Y_T} \right)^2} + p_{vp}^+ \frac{\sigma_{22}}{S_{21}} + \frac{\sigma_{11}}{\sigma_{11D}} = 1 \tag{14}$$

4. Matrix failure in moderate in-plane transverse compression

$$\frac{1}{S_{21}} \left(\sqrt{\tau_{21}^2 + (1 - p_{vp}^- \sigma_{22})^2} + p_{vp}^- \sigma_{22} \right) + \frac{\sigma_{11}}{\sigma_{11D}} = 1 \tag{15}$$

5. Matrix failure in large in-plane transverse compression

$$\left[\left(\frac{\tau_{21}}{2(1 + p_{vv}^-) S_{21}} \right)^2 + \left(\frac{\sigma_{22}}{Y_C} \right)^2 \right] \left(\frac{Y_C}{-\sigma_{22}} \right) + \frac{\sigma_{11}}{\sigma_{11D}} = 1 \tag{16}$$

2.1.3 Material property degradation model (MPDM)

The material property degradation models account for the degradation in material and stiffness properties of the failed plies of an element by decreasing the stiffness values. Two of the widely used models are the sudden (immediate) degradation and the gradual degradation. In the sudden degradation scheme, once a non-linear analysis is performed and the failure of a ply of an element is detected based on the stress analysis of a converged equilibrium solution for a given load level as in Section 2.1.1, the material properties of the failed ply at the integration points are degraded to a small fraction of the undamaged properties only once. It allows to calculate the stiffness of the structure and re-establish equilibrium without several iterations at the same load level. This is because the structure is in linear elastic (Garnich and Akula 2009) regime now where the failed plies carry only a partial amount of the load due to the reduction of the stiffness properties to a small constant value only once. Also, after the implementation of the sudden degradation MPDM and re-establishing equilibrium once, if no failure of the plies of any elements is detected, the load can be incremented to a higher value as in Step 6 and the process can be repeated until structural failure occurs.

On the other hand, the properties of the failed ply of an element are reduced gradually as a function of some evolving field variables such as strain in gradual degradation scheme. This indicates that the ply of an element is allowed to fail repeatedly until the degradation factor R starting from a high value of about 0.5 is reduced to a negligible value in the gradual degradation. In addition, since the stiffness of the laminate is changing continuously due to a gradual change of the degradation factor and the material properties, this requires several iterations even though no new failure

of the plies is detected for a given load level (Garnich and Akula 2009). Therefore, the sudden degradation scheme is computationally efficient because of the need to re-establish equilibrium only once after the detection of the failure of a ply of an element compared with multiple times in the gradual degradation. Hence, the sudden degradation scheme has been used in our study.

Fiber failure

$$(E_{11}^d, G_{12}^d, G_{13}^d, \nu_{12}^d) = R * (E_{11}^0, G_{12}^0, G_{13}^0, \nu_{12}^0) \tag{17}$$

Matrix failure

$$(E_{22}^d, G_{12}^d, G_{23}^d, \nu_{21}^d) = R * (E_{22}^0, G_{12}^0, G_{23}^0, \nu_{21}^0) \tag{18}$$

One of the advantages of using a mode-dependent failure criterion with MPDM is that the material/stiffness of the plies can be reduced accordingly depending on the failure of fiber or matrix as given in (17–18). For example, the material properties associated with the behavior of fiber can be reduced when the mode of failure is fiber failure, whereas the properties associated with the behavior of the matrix can be reduced when the mode of failure is matrix failure as given in (17–18). Here, R represents the residual stiffness factor with a value in the range of 0 to 1 (i.e., $0 \leq R \leq 1$), and a value of 0 indicates a complete failure, whereas a value of 1 indicates no failure. Usually, a value of 0.001–0.01 is used instead of 0 to indicate failure and to avoid the numerical instabilities that restrict the convergence of the solution. Also, the superscript “ d ” indicates the damaged properties whereas “0” indicates the undamaged properties of the materials. In some studies, only the modulus of the failed plies materials is degraded upon failure and Poisson’s ratio is not degraded (Tan and Nuismer 1989; Tan and Perez 1993; Garnich and Akula 2009), and a similar approach has been used in our study. Once the degraded material properties are calculated, the reduced stiffness components of the failed plies in (4), which are dependent on material properties, can be modified using the degraded material properties and further analysis can be carried out.

For this study, the properties of the failure criterion and MPDM required for PFA were supplied to the MSC Nastran software by developing a subroutine in MATLAB.

3 Uncertainty propagation and global sensitivity analysis using polynomial chaos expansion

3.1 Theory for polynomial chaos expansion

Polynomial chaos expansion (PCE) is a high accuracy uncertainty propagation technique that was first proposed

by Wiener in his work *The Homogeneous Chaos* in 1938 (Wiener 1938). In PCE, a second-order random process $u(z, t, \vec{\xi})$ is represented as a spectral expansion in terms of multivariate orthogonal polynomials $\psi_k(\cdot)$ and deterministic PCE coefficients a_k as in (19).

$$u(z, t, \vec{\xi}) = \sum_{k=0}^{\infty} a_k(z, t) \cdot \psi_k(\vec{\xi}) \tag{19}$$

$$u(\vec{\xi}) \approx \sum_{k=0}^P a_k \cdot \psi_k(\vec{\xi}) \tag{20}$$

$$P + 1 = \binom{p + N}{N} = \frac{(p + N)!}{p!N!} \tag{21}$$

In (19), $z \in \mathbb{R}^d$ ($d = \{1, 2, 3\}$) represents the spatial term, t represents the time, and $\vec{\xi} = \{\xi_i\}_{i=1}^N$ represents the set of N -independent standard random variables, which has a one-to-one correspondence with original random input variables $x = \{x_i\}_{i=1}^N$. Using a total order expansion scheme for truncation of the infinite series in PCE, the PCE can be expressed as in (20) and the total number of PCE terms for a PCE of order p with N random inputs is given in (21).

In PCE, multivariate orthogonal polynomials $\psi_k(\cdot)$ are generated by taking the tensor product of the univariate orthogonal polynomials $\phi_{\alpha_i^k}(\xi_i)$ as given in (22), where α_i^k are termed as multi-indices which represent the order of the univariate orthogonal polynomials. The expression for multi-indices using a total order expansion for a PCE of order p with N random inputs is given in (23).

$$\psi_k(\vec{\xi}) = \prod_{i=1}^N \phi_{\alpha_i^k}(\xi_i) \tag{22}$$

$$\alpha_p^N = \left\{ \alpha \in \mathbb{N}^N : 0 \leq \sum_{i=1}^N \alpha_{(i)} \leq p \right\} \tag{23}$$

In PCE, the Askey Scheme (Xiu and Karniadakis 2002; Szeg 1939; Gautschi 2004) can be adopted for the selection of orthogonal polynomials based on the distribution of random inputs. For instance, hermite polynomials can be used for normal random variables.

One of the main steps in developing PCE approximation is the estimation of PCE coefficients a_k . To this end, a non-intrusive approach based on regression using least-squares, as discussed in the next subsection, has been used in this study. The advantage of using a non-intrusive method is that commercial finite element analysis (FEA) software can be used as a black-box for UQ, and it does not require an additional modification of deterministic codes. Once the PCE coefficients are calculated, an explicit relation between the random inputs and the stochastic response

is known. Furthermore, the mean and variance of the stochastic response can be calculated analytically as in (24).

$$\begin{aligned} \mu_u &= E \left[u \left(\vec{\xi} \right) \right] = a_0 \\ \sigma^2_u &= \text{Var} \left(u \left(\vec{\xi} \right) \right) = \sum_{k=1}^P a_k^2 \mathbb{E} \left[\psi_k^2 \right] \end{aligned} \tag{24}$$

3.2 Regression using least-squares (stochastic point collocation)

Stochastic point collocation or simply COLLOC is based on fitting the response at the given sampling points and involves the minimization of mean-square error of PCE approximation (Hosder et al. 2006; Hosder et al. 2010; Choi et al. 2006; Thapa et al. 2018b; 2019c; 2020). The PCE approximation using regression can be given as in (25).

$$y \approx u \left(\vec{\xi} \right) = \psi^T \hat{a} \tag{25}$$

In (25), $\psi^T = \{1 \ \psi_1 \ \psi_2 \ \dots \ \psi_P\}$ represents multivariate orthogonal polynomials evaluated at the sampling points and $\hat{a} = \{a_0, a_1, \dots, a_P\}^T$ represents PC coefficients. So, for a given design of experiments (DOE) $\chi = \{\xi^{(1)}, \dots, \xi^{(n_s)}\}^T$ with size n_s and corresponding function evaluations $Y = \{y^{(1)}, \dots, y^{(n_s)}\}^T$, (23) can be expressed as in (26) where $\Psi_{ij} = \psi_j \left(\xi^{(i)} \right)$. It is suggested that the number of samples should be greater than the number of PCE terms, i.e., $n_s > (P + 1)$ to avoid over-fitting.

$$\Psi \hat{a} = Y \tag{26}$$

Using the least-squares approach, the linear regression coefficients can be estimated using (27) where $\Psi^T \Psi$ is known as the information matrix.

$$\hat{a} = \left(\Psi^T \Psi \right)^{-1} \Psi^T Y \tag{27}$$

Note that some of the most recent approaches for PCE include the L_1 -minimization and least-angle regression (LARS) techniques which are found to be capable of yielding sparse solution containing only few PCE terms as well as yielding PCE solutions even for the under-determined system when the number of samples is less than the number of PCE terms (Thapa et al. 2018b). However, the L_1 minimization requires extra computational effort in estimating regularization parameters whereas LARS is based on solving a least-squares problem iteratively by adding basis polynomials successively for multiple times, which becomes time-consuming when the number of PCE terms is huge. Furthermore, the sparsity of the underlying basis space is rarely known a priori, and it would require a similar number of samples as the number of PCE terms when the sparsity of the basis space is low. Therefore, the

least-squares-based approach using total order expansion was given priority in this study due to simplicity and efficiency in terms of processing time.

3.3 Global sensitivity analysis using polynomial chaos expansion

The main goal of performing global sensitivity analysis (GSA) is to estimate the influence of random inputs on the variation of stochastic responses (Saltelli et al. 2000; Sudret 2008; Crestaux et al. 2009). Mostly, the GSA is performed with the variance-based method by performing Sobol decomposition of the variance of the stochastic response. In this method, the sensitivity of random inputs is measured using Sobol indices for which MCS used to be the preferred approach. However, the MCS based approach becomes computationally infeasible when the number of random input variables is too high. On the other hand, the PCE based Sobol indices can be calculated during a post-processing step once the PCE coefficients are estimated, and the total number of samples required is only equal to that required for PCE construction which is substantially less than the MCS approach. Hence, the GSA using PCE-based Sobol indices is performed in this study.

Based on (23), let J_{i_1, \dots, i_s} define the subset of multi-indices α_p^N such that the only non-zero terms are $\{\alpha_{i_1}, \dots, \alpha_{i_s}\}$ as given in (28).

$$J_{i_1, \dots, i_s} = \left\{ \alpha^{(k)} : \begin{array}{ll} \alpha_j > 0 & \forall j = 1, \dots, N, \quad j \in (i_1, \dots, i_s) \\ \alpha_j = 0 & \forall j = 1, \dots, N, \quad j \notin (i_1, \dots, i_s) \end{array} \right\} \tag{28}$$

where, $k = 0, 1, \dots, P$

Rearranging the terms in (20) such that J_{i_1, \dots, i_s} correspond to the polynomials that are dependent on only $\xi_{i_1}, \dots, \xi_{i_s}$, the PCE of a random response $u \left(\vec{\xi} \right)$ can be expressed in the form of Sobol decomposition as in (29).

$$\begin{aligned} u \left(\vec{\xi} \right) &= a_0 + \sum_{i=1}^N \sum_{\alpha \in J_i} a_\alpha \psi_\alpha \left(\xi_i \right) + \sum_{1 \leq i_1 < i_2 \leq N} \sum_{\alpha \in J_{i_1, i_2}} a_\alpha \psi_\alpha \left(\xi_{i_1}, \xi_{i_2} \right) \\ &+ \sum_{1 \leq i_1 < \dots < i_s \leq N} \sum_{\alpha \in J_{i_1, \dots, i_s}} a_\alpha \psi_\alpha \left(\xi_{i_1}, \dots, \xi_{i_s} \right) \tag{29} \\ &+ \dots + \sum_{\alpha \in J_{1, \dots, N}} a_\alpha \psi_\alpha \left(\xi_1, \dots, \xi_N \right) \end{aligned}$$

Similarly, Sobol decomposition of the total variance of the response can be written as in (30).

$$\begin{aligned} D &= \text{Var} \left[u \left(\vec{\xi} \right) \right] \\ &= \sum_{i=1}^N D_i + \sum_{1 \leq i < j \leq N} D_{ij} + \dots + D_{1,2, \dots, N} \end{aligned} \tag{30}$$

So, the PCE-based Sobol Indices which represent the ratio of the partial variance D_{i_1, \dots, i_S} to the total variance of the response PCE D or σ^2_u can be given as in (29).

$$S_{i_1, \dots, i_S} = \frac{D_{i_1, \dots, i_S}}{D} = \frac{\sum_{\alpha \in J_{i_1, \dots, i_S}} \alpha^2 \mathbb{E}[\psi^2_\alpha]}{D} \quad (31)$$

$$J_i = \left\{ \alpha^{(k)} : \begin{array}{ll} \alpha_j > 0 & \forall j = 1, \dots, N, \quad j = i \\ \alpha_j = 0 & \forall j = 1, \dots, N, \quad j \neq i \end{array} ; k = 0, 1, \dots, P \right. \quad (32)$$

$$J_i^T = \left\{ \alpha^{(k)} : \begin{array}{ll} \alpha_j > 0 & \forall j = 1, \dots, N, \quad j = i \\ \alpha_j \geq 0 & \forall j = 1, \dots, N, \quad j \neq i \end{array} ; k = 0, 1, \dots, P \right. \quad (33)$$

Based on the Sobol decomposition in (29-30), there are $2^N - 1$ partial variances of the response, which becomes enormous for problems with a large number of random inputs. Hence, two of the sensitivity indices that are generally of interest are the first-order and total sensitivity indices. The first-order index S_i (also known as the main effect) of a random variable represents its variance contribution when considered alone whereas the total sensitivity index S_i^T (also known as the total effect) represents its variance contribution while considering the contribution of other random inputs (mixed interactions) as well. Hence, the multi-indices set for first-order Sobol indices J_i and total Sobol indices J_i^T can be given as in (32) and (33), respectively. Upon using the partial variance of the PCE terms based on these multi-indices in (31), the corresponding Sobol indices can be obtained.

4 Stochastic progressive failure analysis of composite structures with polynomial chaos expansion

Based on the discussions related to composites and PCE in previous sections, a stochastic framework was developed, as shown in Fig. 2 so that the uncertainty analysis for a complex non-linear problem of composite structures can be carried out at an affordable computational cost. For this study, the stochastic framework and the subroutines—to pass the information regarding the failure criterion and MPDM for pre-processing to FEA solver and extract the selected information from a huge data file of the FEA results for post-processing—were written in MATLAB. Also, the MSC Nastran software was used as a FEA solver.

First of all, the framework begins with defining a problem by obtaining a deterministic FEA model to carry out PFA and selecting the random inputs as well as random responses for uncertainty analysis. Here, the material properties, geometric properties, and loading conditions can be selected as random inputs, whereas the FPF load, ultimate load, LPF load, and so on can be selected as random outputs. In the second step, the statistical information for

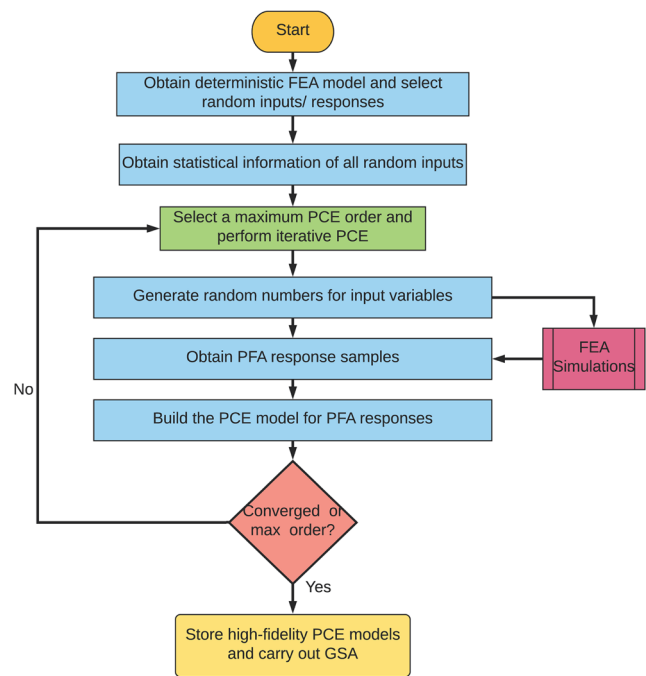


Fig. 2 Framework for uncertainty quantification and global sensitivity analysis for the progressive failure of fiber-reinforced composites

the random inputs is provided based on the available data or is selected based on expert opinions. Then, a maximum order for PCE is selected so that convergence analysis of the PCE can be carried out starting from the first-order PCE. During the first iteration, a first-order PCE is selected and a set of random samples is generated for the random inputs such that its size is greater than the number of PCE terms using (21). It is followed by running the PFA using FEA for each realization of the random inputs and then obtaining the response samples. These samples are then used to estimate the PCE coefficients as given in (27), and the statistics, as well as the probability density function (PDF) using a random sampling of the stochastic responses, are estimated. Most importantly, the accuracy of the developed PCE models should be assessed at the new sampling points that are unused for PCE construction. Hence, a cross-validation sample set of 100 samples is used to calculate the relative mean square error (RMSE) using (34) where n_{VS} is the number of validation samples, u_{exact} is the exact response obtained from FEA simulations, and u_{PCE} is the response calculated with PCE model. After calculating the statistics and RMSE of the PCE, the accuracy of the PCE is assessed and the order of PCE is increased. Onwards second order, if the convergence of the statistics or RMSE is obtained, the framework exits the iterative PCE approximation loop and performs the GSA by estimating Sobol indices using high fidelity PCE as in Section 3.3. Contrarily, if the convergence is not observed, then the iterative loop continues until the convergence or the maximum PCE order is attained.

Note that the LASSO, LARS, and L_1 minimization techniques as discussed in Section 3.2 can also be integrated into this framework. The L_1 minimization technique was also tested with this framework; however, there were no substantial computational savings in terms of the number of FEA simulations compared with the COLLOC, so the COLLOC technique was utilized for the application problems.

$$RMSE = \frac{\sum_{i=1}^{n_{VS}} \left(u_{exact}(\xi^{(i)}) - u_{PCE}(\xi^{(i)}) \right)^2 / n_{VS}}{\sum_{i=1}^{n_{VS}} \left(u_{exact}(\xi^{(i)}) - \mu_u \right)^2 / n_{VS}} \quad (34)$$

where, $\mu_u = \sum_{i=1}^{n_{VS}} u_{exact}(\xi^{(i)}) / n_{VS}$

5 Applications and discussions

The presented framework for stochastic PFA and GSA of composite structures was applied to a composite laminate with circular cutout subjected to different load cases under the presence of uncertainties in material properties. And, the results, along with the discussions, are provided in this section.

5.1 Model description and validation of a deterministic FEA model

Before performing a stochastic analysis, it is essential to validate the FEA-based PFA with FEA software to

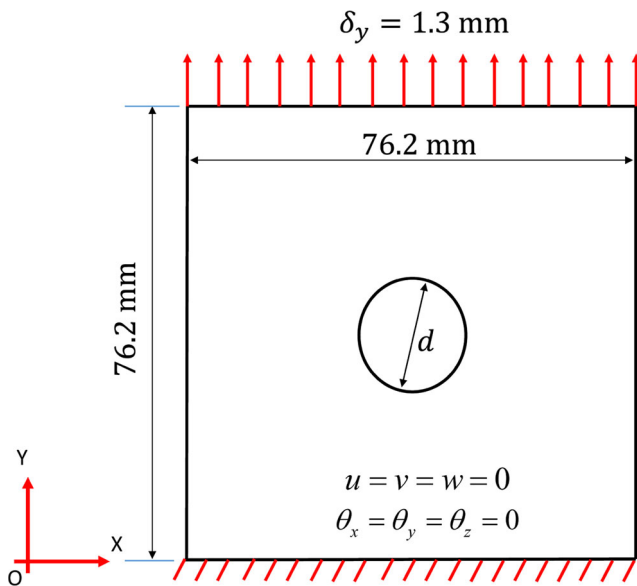


Fig. 3 The geometry of a composite laminate with circular cutout used for validation

Table 1 The material properties of an IM7/5250-4 carbon/epoxy composite

Elastic modulus in the longitudinal direction, E_{11} (GPa)	172.4
Elastic modulus in the transverse direction, E_{22} (GPa)	10.3
Shear modulus, $G_{12} = G_{13}$ (GPa)	5.52
Shear modulus, G_{23} (GPa)	3.45
Poisson's ratio, $\nu_{12} = \nu_{13}$	0.32
Poisson's ratio, ν_{23}	0.4
Longitudinal tensile strength, X_T (MPa)	2526.5
Longitudinal compressive strength, X_C (MPa)	1620
Transverse tensile strength, $Y_T = Z_T$ (MPa)	65.5
Transverse compressive strength, $Y_C = Z_C$ (MPa)	248
Shear strength, $S_{12} = S_{13}$ (MPa)	122
p_{vp}^+	0.35
$p_{vp}^- = p_{vv}^-$	0.3

be used as a black box in uncertainty studies. To this end, a composite laminate with a circular cutout as given in Fig. 3 was considered since most of the aerospace structures consist of fastener holes. Also, this laminate was considered by Liu et al. using the Plate Element-Failure Method for deterministic PFA in(Liu et al. 2010).

The laminate considered in Fig. 3 is a carbon/epoxy quasi-isotropic laminate with a stacking sequence of $[+45^0/0^0/-45^0/90^0]_S$, where the ply orientation is considered with respect to the y -axis (i.e., 0^0 plies are oriented along the y -axis in the loading direction) (Liu et al. 2010) for validation of FEA software-based PFA. It has a length and width of 76.2 mm and 76.2 mm, respectively, whereas the thickness of each ply is 0.125 mm. The

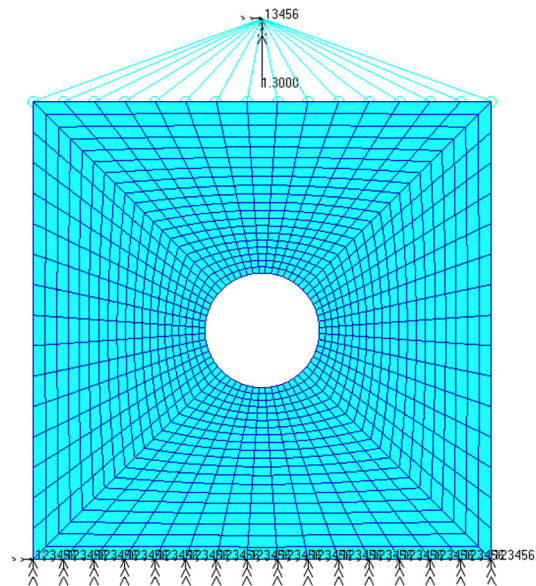


Fig. 4 The optimal mesh of a composite laminate with circular cutout used for validation (1200 QUAD4 shell elements)

Table 2 The comparison of the ultimate strength obtained with PFA using FEA for validation in this study to that provided in the literature

Experimental (MPa)	Reference (Liu et al. 2010) (MPa)	Current study (MPa)
397.1	382.3	388.91

diameter of the circular cutout at the center is 19.05 mm, and the material properties of the composite are provided in Table 1. Also, RBE2 elements were used at the upper edge of the laminate to create a multi-point constraint as in Fig. 4 for uniform loading along the edge, and a displacement control method with a final displacement $\delta_y = 1.3$ mm was used along the y-axis. The PFA was then carried out using Puck’s failure criterion and a sudden degradation scheme with a value of 0.01 for residual stiffness factor ($R = 0.01$). The best results for the ultimate strength of the laminate obtained with a mesh convergence analysis are provided in Table 2 which resulted in mesh size of 1200 QUAD4 shell elements, as shown in Fig. 4. Note that it is challenging to find a perfect match between the numerical results of PFA and experimental results since the numerical simulations are hugely affected by a plethora of factors such as the failure criterion, degradation model, and degradation factor. Nonetheless, the study for the PFA of this laminate using FEA yielded similar results to that of experimental data and that of Liu et al. (2010) in Table 2 and suggested the validity of the FEA-based PFA using MSC Nastran. The geometry and the FEA mesh from the validation study were then used for the stochastic study by considering the material coordinate system coincident with the global coordinate system (i.e., 0^0 and 90^0 plies along the global x-axis and y-axis, respectively) since the similar response behavior of the laminate with the coordinate system as in Liu et al. (2010) was obtained with this new material coordinate system. This was also done in part to be consistent with most of the

books and literature on composites.

Most importantly, performing PFA using FEA is a computationally costly process, and it required approximately 6 min to run a single simulation using a computer with Intel(R) Xeon (CPU E5-1620 v3 @3.5GHz processor and 16 GB RAM configuration). Therefore, it demands an efficient approach, such as PCE for UQ, which requires fewer number of FEA calls.

In the subsequent subsections, the validated FEA model with optimal mesh size was considered to study the effects of uncertainties in material properties on the FPF and ultimate failure displacements and corresponding loads denoted as δ_{FPF} , P_{FPF} , δ_{ULT} , and P_{ULT} respectively. So, the material properties in Table 1 were considered to be random, having a Gaussian distribution with a coefficient of variation (COV) of 0.1 from the mean values provided in Table 1 thereby accounting for a total of eleven random variables.

5.2 Composite laminate with a circular cutout subjected to in-plane uniaxial tension

The stochastic framework was at first applied to a laminate that has a stacking sequence of $[45^0/0^0/-45^0/90^0]_s$ with respect to the global coordinate system in Fig. 3 and was subjected to tensile loading. The deterministic simulation about the mean values of the random inputs was performed and the failure progression is displayed in Fig. 5, which indicates that the failure started in the vicinity of the hole

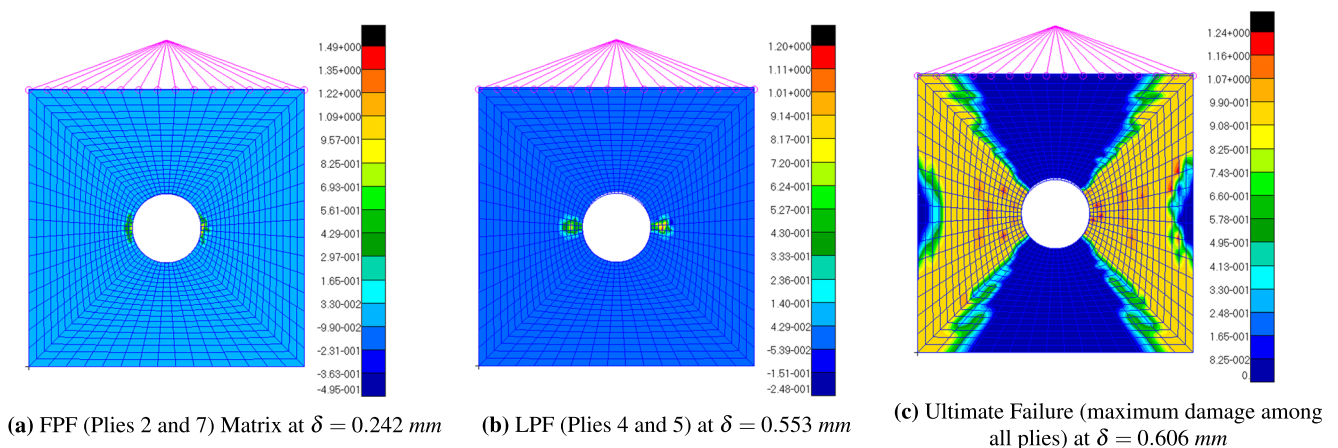


Fig. 5 Damage progression of a composite laminate with circular cutout subjected to in-plane uniaxial tensile loading (a value of greater than 1 in the color bar suggests a failure)

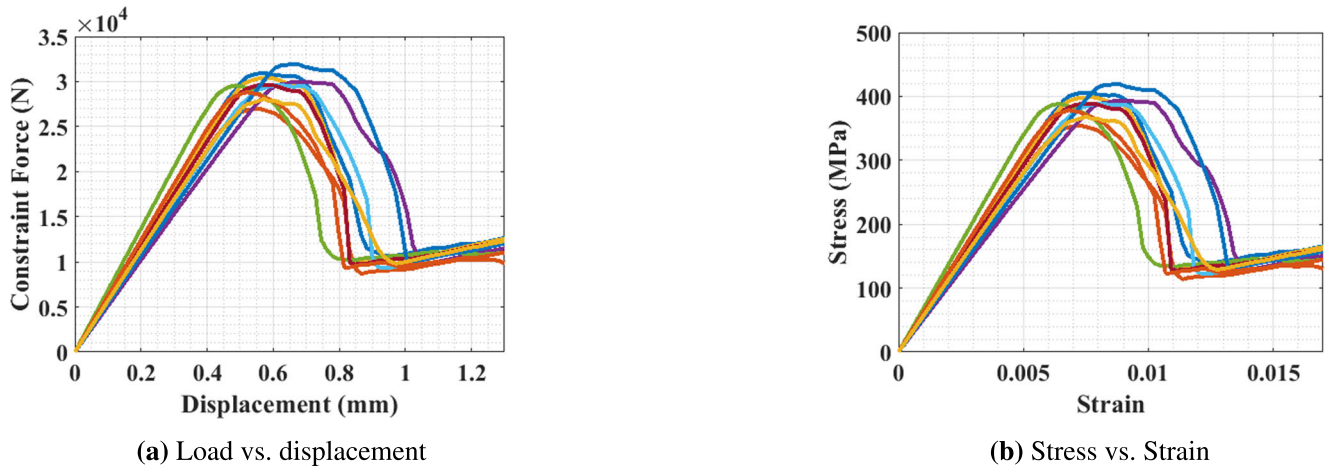


Fig. 6 The stochastic nature of the non-linear responses of a composite laminate during PFA under the presence of uncertainties in material properties

Table 3 The statistics for the PFA responses under uniaxial in-plane tension using stochastic approach

Response			δ_{FPF} (mm)	P_{FPF} (N)	δ_{ULT} (mm)	P_{ULT} (N)
LHS simulation (5000 samples)	Mean		2.39E-01	1.38E+04	5.95E-01	2.95E+04
	Std		3.37E-02	2.25E+03	6.54E-02	2.29E+03
PCE	Order =2 (306 samples)	Mean	2.39E-01	1.38E+04	5.95E-01	2.95E+04
		Std	3.39E-02	2.27E+03	6.37E-02	2.29E+03
	Order =3 (498 samples)	Mean	2.39E-01	1.38E+04	5.96E-01	2.95E+04
		Std	3.34E-02	2.26E+03	6.71E-02	2.29E+03

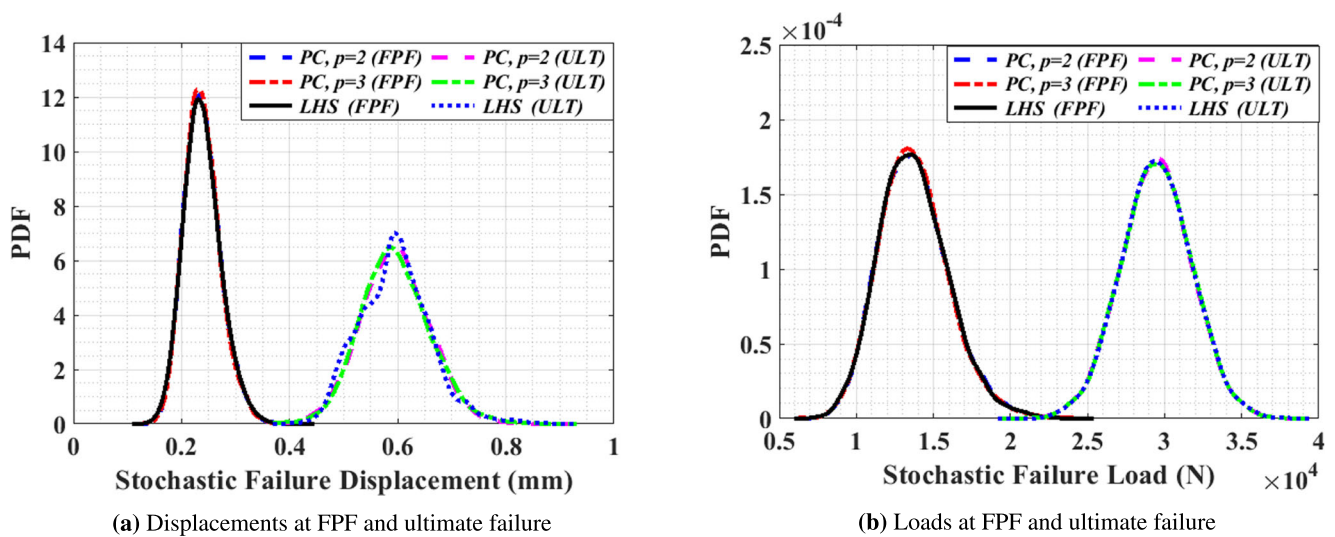


Fig. 7 The PDF plots of the stochastic responses of a composite laminate with a circular cutout subjected to uniaxial in-plane tension

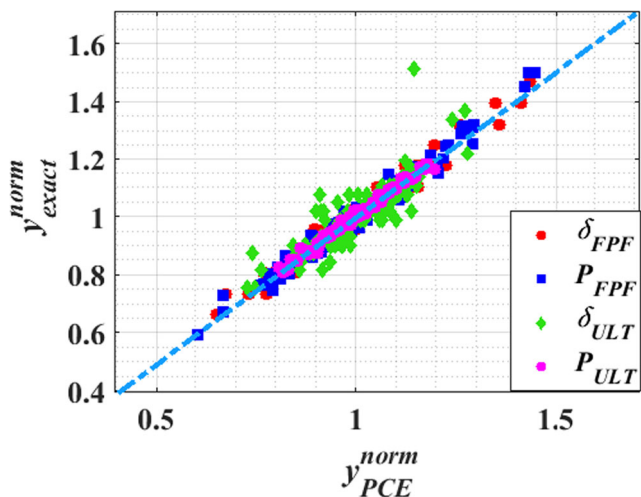


Fig. 8 The normalized cross-validation plot of the stochastic responses with PCE for a composite laminate with a circular cutout subjected to uniaxial in-plane tension (the normalization was carried out dividing the response values with their corresponding mean values)

in the plies 2 and 7 (with a ply orientation of 0^0) and perpendicular to the tensile loading direction. The mode of FPF was observed to be matrix failure in tension, which was followed by the progression of failure in other plies, and the LPF occurred before the ultimate failure with the failure contributed by both fiber and matrix failure. Mainly, the damage was observed to be more widespread during the ultimate failure and is primarily due to the fiber rupture of 90^0 plies with fiber oriented along loading direction. The values of δ_{FPF} , P_{FPF} , δ_{ULT} , and P_{ULT} were found to be 0.242 mm, 13,993.418 N, 0.6066 mm, and 29,635.029 N, respectively.

Upon considering the randomness in material properties, the effects on the load-displacement behavior of the laminate, and hence the failure responses, are evident with the dissimilar curves for different realizations of the random inputs in Fig. 6. So, the PCE was constructed for the four responses δ_{FPF} , P_{FPF} , δ_{ULT} , and P_{ULT} using the

framework in Fig. 2 and the summary of probabilistic responses is provided in Table 3. To demonstrate the accuracy and computational efficiency of PCE, the results obtained with 5000 LHS simulations are also provided. The similar results of PCE with a fewer number of samples, as opposed to 5000 Latin hypercube sampling (LHS) simulations, underlines the benefits of PCE. The high accuracy of the converged PCE models is also demonstrated by the almost identical PDF plots of PCE and LHS simulations for failure responses in Fig. 7 and the linear trends in the cross-validation plot in Fig. 8. The RMSE values of the PCE response using validation samples as in Fig. 8 were in the range of 0.01 to 0.2 which indicated a high prediction accuracy. In Fig. 7, the location of the mean of the PDF of ultimate failure is at a higher value than that of FPF as expected and the farther apart location of the FPF and ultimate failure response PDFs with very small overlapping suggests a stable damage progression dominated by matrix failure. Furthermore, similar PDFs of PCE with chaos orders 2 and 3 indicate the convergence of PCE as well which can then be utilized for GSA.

The total Sobol index plots for the FPF and ultimate failure responses are provided in Figs. 9 and 10, and the values of Sobol indices are found to be unique for different responses, thereby indicating an unequal contribution of the random inputs for different responses. In these plots, lower tolerance value of 0.01 (indicated with a dotted black line) and higher tolerance of 0.1 (indicated with a dotted magenta line) were specified so that the random inputs with Sobol indices lower than 0.01 can be declared as negligible random inputs (deterministic for future studies or model refinement) and those with values greater than 0.1 can be selected as highly significant random inputs, respectively. The random inputs with Sobol indices in between lower and higher tolerances were specified to have a moderate contribution. Doing so, the number of negligible random inputs was found to be approximately seven except for δ_{ULT} which included all Sobol indices with values greater than the lower tolerance.

Fig. 9 Total Sobol indices for FPF and ultimate failure displacements of a composite laminate with a circular cutout subjected to uniaxial in-plane tension

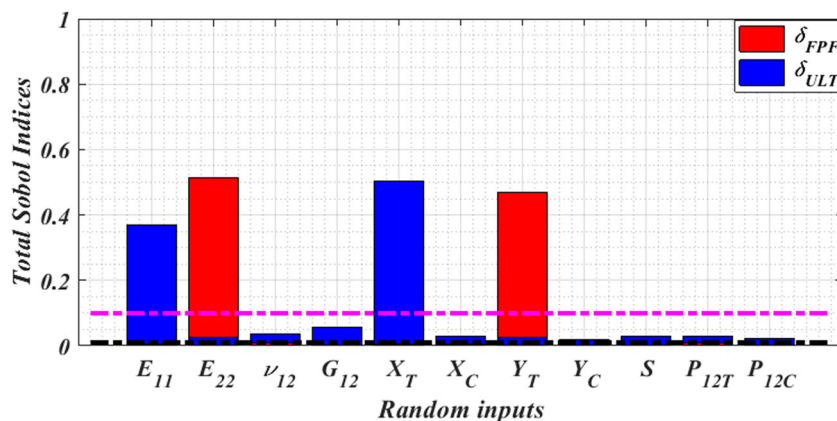
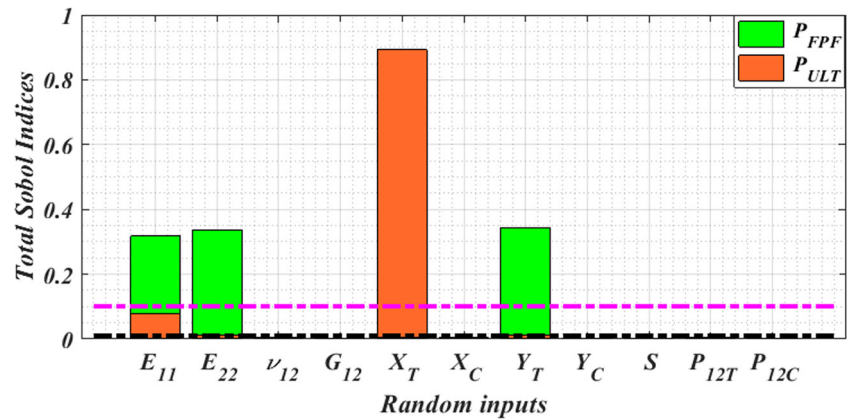


Fig. 10 Total Sobol indices for FPF and ultimate failure loads of a composite laminate with a circular cutout subjected to uniaxial in-plane tension



On the other hand, the number of highly significant random inputs was in the range of 1 to 3. Moreover, the Sobol indices of E_{22} and Y_T were found to have large values than the other random inputs for δ_{FPF} and P_{FPF} since the FPF failure is due to matrix failure in tension whereas that of E_{11} and X_T were found to be high for δ_{ULT} and P_{ULT} , thereby indicating the ultimate failure is highly influenced by fiber failure in tension. Therefore, an intuitive connection between the Sobol indices of the failure responses and failure modes was clearly observed for the given laminate subjected to tensile loading.

It is to be noted that the FEA modeling approach utilized here is based on the stress–strain state (for failure detection) and sudden degradation (for MPDM), which requires ply level properties only and does not involve fracture toughness. This approach was considered since a majority of studies on PFA, as mentioned in Section 1, have adopted this approach due to its computational efficiency, and it also yielded similar results to that of experiments during validation. Alternatively, the strength prediction of notched composite laminates can also be carried out using the approaches, mainly based on fracture mechanics, that

account for the fracture toughness (Camanho et al. 2007; Vallmajó et al. 2019). So, a comparative analysis of the strength predictions with and without fracture toughness under uncertainty presents a future scope of this study.

5.3 Composite laminate with a circular cutout subjected to uniaxial in-plane compression

The composite laminate with a circular cutout in Section 5.2 with material coordinate system coincident with the global coordinate system was also considered for uniaxial in-plane compressive loading. To this end, a displacement control method was used with a final displacement of $\delta_y = -0.6$ mm for the top edge along negative y-direction opposite to that of the tensile loading direction. As shown in Fig. 11, the failure started near the edge of the cutout perpendicular to the compressive loading direction similar to that in the tensile case. However, for the compressive loading, the FPF mode was fiber failure under compression in plies 4 and 5 due to these plies carrying a significant amount of load as the fiber is oriented parallel to the loading direction. Also, the ultimate failure was observed due to the

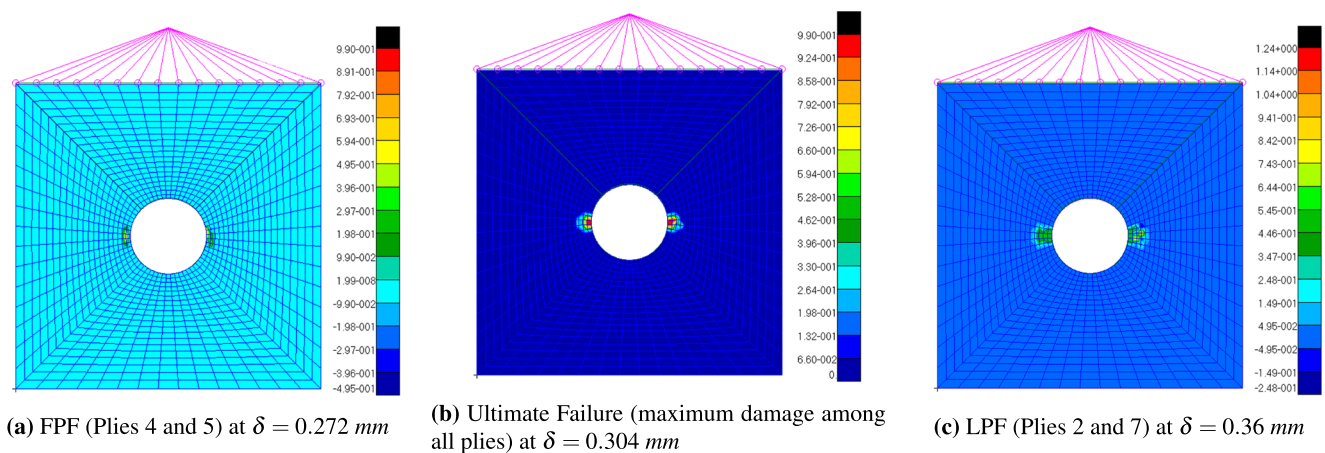


Fig. 11 Damage progression of a composite laminate with circular cutout subjected to in-plane compressive loading

Table 4 The statistics for the PFA responses under uniaxial in-plane compression with the stochastic approach

Response			δ_{FPF} (mm)	P_{FPF} (N)	δ_{ULT} (mm)	P_{ULT} (N)
LHS simulation (5000 samples)	Mean		2.73E-01	1.52E+04	3.12E-01	1.71E+04
	Std		3.79E-02	1.56E+03	4.03E-02	1.49E+03
PCE	Order =2 (156 samples)	Mean	2.73E-01	1.52E+04	3.07E-01	1.71E+04
		Std	3.82E-02	1.55E+03	3.99E-02	1.37E+03
	Order =3 (498 samples)	Mean	2.73E-01	1.52E+04	3.10E-01	1.70E+04
		Std	3.83E-02	1.54E+03	3.99E-02	1.43E+03

The table includes the magnitude of the responses without a negative sign for compression

occurrence of compressive fiber failure in more number of elements in plies 4 and 5 than in FPF, and the LPF was found in plies 2 and 7 due to matrix failure under compression after ultimate failure. For deterministic simulation about mean values of the random inputs, the magnitudes of δ_{FPF} , P_{FPF} , δ_{ULT} , and P_{ULT} were found to be 0.272 mm, 15,284.494 N, 0.304 mm, and 17,379.152 N, respectively.

The results obtained from UQ for this compressive loading case by considering the randomness in material properties, as given in Section 5.2, are provided in Table 4. The results obtained with 498 samples for third-order PCE are almost similar to those obtained with 5000 LHS simulations, and it yielded a maximum value of absolute percentage error less than 1 and 5 for the mean and standard deviation of the response, respectively. The high accuracy of PCE is also evident from the identical PDF plots obtained with PCE and 5000 LHS simulations in Fig. 12. Interestingly, the locations of the FPF and ultimate failure PDFs are too close than in the tensile case which indicates an abrupt transition from the FPF to ultimate failure. It can be attributed to the fiber failure dominated

failure progression which is more unstable than the matrix dominated failure progression in the tensile case. Also, the RMSE obtained with 100 cross-validation samples was in the range of 0.03 to 0.9, which indicated a high prediction accuracy that is also evident by the almost linear trends in Fig. 13 for three of the responses except δ_{ULT} for which some scatter is apparent. Nonetheless, most of the predictions of δ_{ULT} followed the linear pattern, and hence the results were accepted.

The third-order PCE obtained from convergence analysis was then utilized to estimate the total Sobol indices, as shown in Figs. 14 and 15, and the tolerance values for Sobol indices as in tensile loading was used here as well. It is clear from the Sobol indices of δ_{FPF} and P_{FPF} that the FPF is massively influenced by E_{11} and X_C since the FPF, which indicates the transition from linear to non-linear response, is dominated by fiber failure under compression. Also, the major influence of E_{11} and X_C on δ_{ULT} and P_{ULT} supports the indication that the failure mode identified by the deterministic simulation during an ultimate failure is fiber failure under compression.

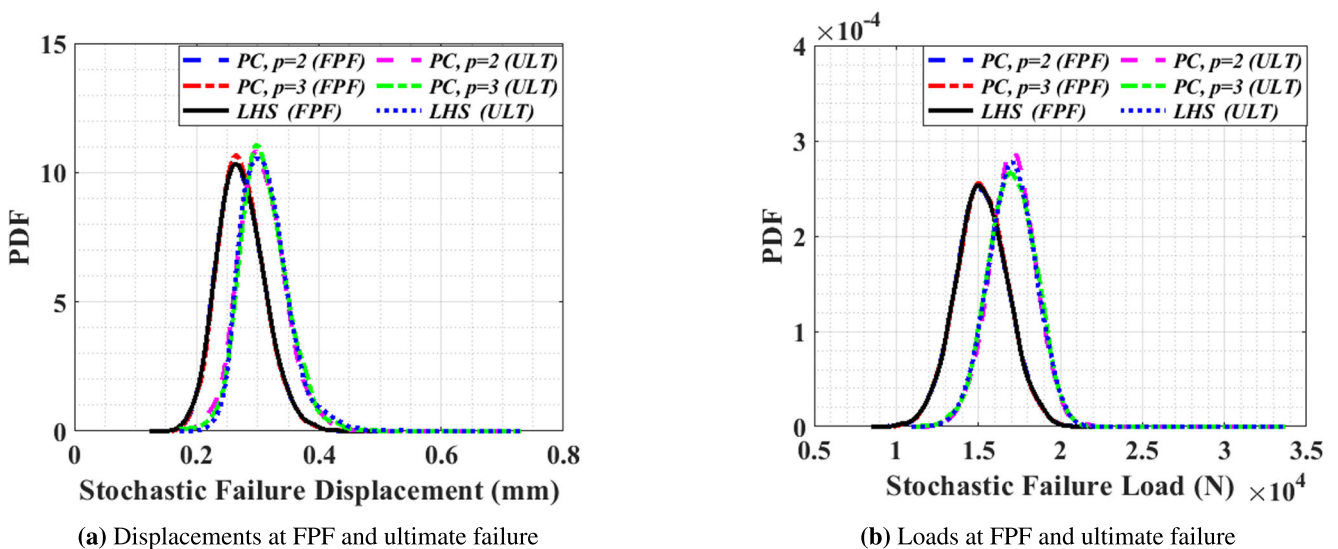


Fig. 12 The PDF plots of the stochastic responses of a composite laminate with a circular cutout subjected to uniaxial in-plane compression

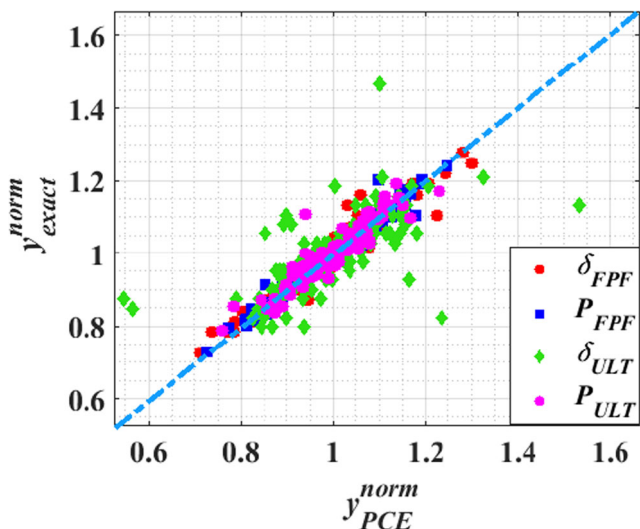


Fig. 13 The normalized cross-validation plot of the stochastic responses with PCE for a composite laminate with a circular cutout subjected to uniaxial in-plane compression (the normalization was carried out dividing the response values with their corresponding mean values)

An improvement over the current FEA model includes the implementation of cohesive zone elements to account for the delamination that would result from micro-buckling under compression (Su et al. 2015). Also, implementing approaches that account for fracture toughness for subsequent in-plane failure propagation after initiation seems interesting. Nonetheless, the same uncertainty quantification framework in Section 4 can be utilized by considering the maximum traction, critical tip displacement, and fracture toughness as random inputs when necessary once a validated FEA model is built.

5.4 Composite laminate with circular cutout subjected to out-of-plane transverse displacement

Finally, the laminate with a circular cutout was considered for out-of-plane transverse loading perpendicular to the

laminate by considering the same stacking sequence and material coordinate system as in Sections 5.2–5.3. Here, all of the four edges of the laminate were simply supported, and the corner nodes were fixed to avoid rigid body motion. The displacement control method was used by creating a multi-point constraint with RBE2 elements connected to the nodes along the circumference of the cutout so that the final displacement of these nodes was $\delta_z = -5.6$ mm out-of-plane of the laminate. The failure progression obtained with the properties in Table 1 is provided in Fig. 16 which shows that the FPF was observed in the bottom layer (ply 1 with 45° orientation) of the laminate due to matrix failure in tension since the bottom layer is in tension. Similarly, the second plot for maximum damage among all plies during ultimate failure shows that the failure is more widespread and reached the corners and edges of the laminate whereas the third plot shows that the LPF was observed due to matrix failure under compression of elements in ply 6 (orientation of -45°) near to the corners of the laminate. For this out-of-plane loading case, the magnitudes of δ_{FPF} , P_{FPF} , δ_{ULT} , and P_{ULT} were found to be 1.760 mm, 384.670 N, 5.060 mm, and 2947.485 N, respectively.

In Table 5, the comparison of the first two moments obtained with PCE and LHS simulations is provided. It is obvious that the results obtained with 928 samples for PCE are similar to that with 5000 LHS simulations, and the maximum absolute percentage difference in the mean value of the responses with PCE and LHS results is about 0.5%, whereas it is about 2% for the standard deviation. Mainly, the number of samples required for this out-of-plane transverse loading is higher than that required for uniaxial tension and compression, and it is due to a higher geometric non-linearity associated with the ultimate failure at a larger displacement for out-of-plane transverse loading. The effect of high non-linearity was also slightly observed in the peak of the PDF plot of δ_{ULT} in Fig. 17a; however, the PDF of the other responses obtained with PCE is similar to that with LHS. Moreover, the validation samples exhibited a linear trend for most of the responses (thereby

Fig. 14 Total Sobol indices for FPF and ultimate failure displacements of a composite laminate with a circular cutout subjected to uniaxial in-plane compression

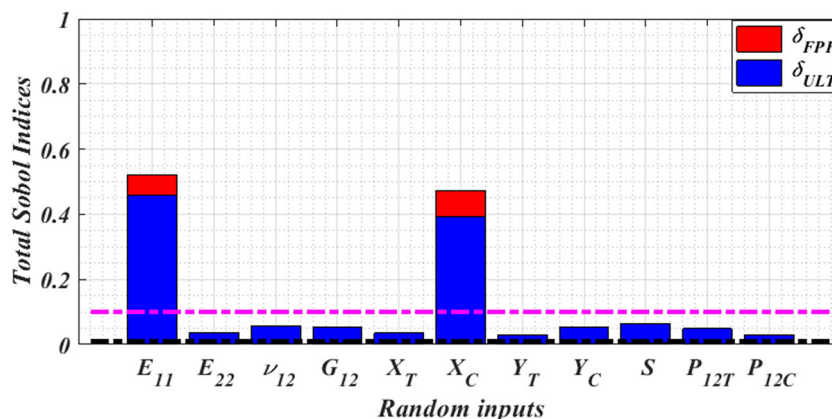


Fig. 15 Total Sobol indices for FPF and ultimate failure loads of a composite laminate with a circular cutout subjected to uniaxial in-plane compression

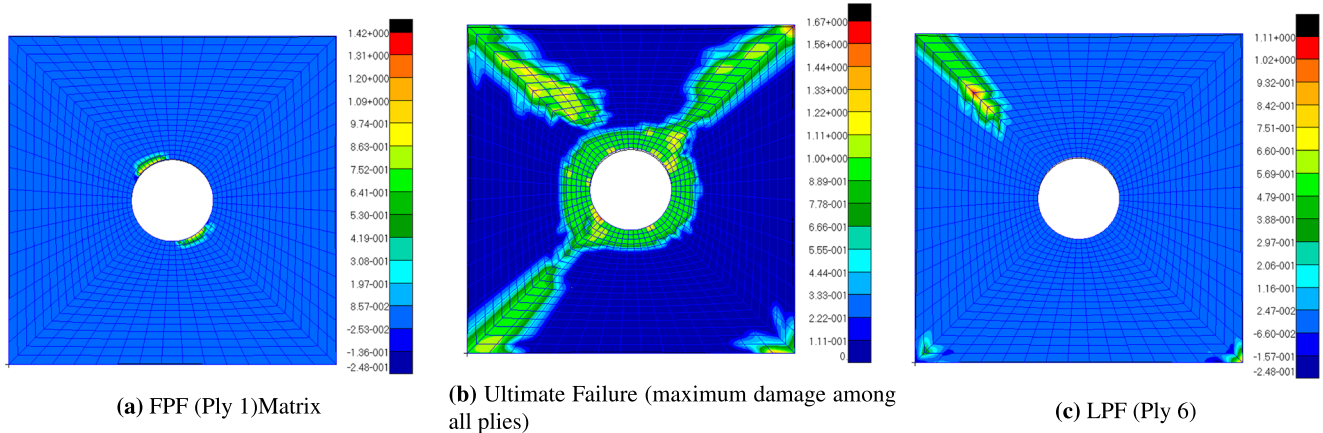
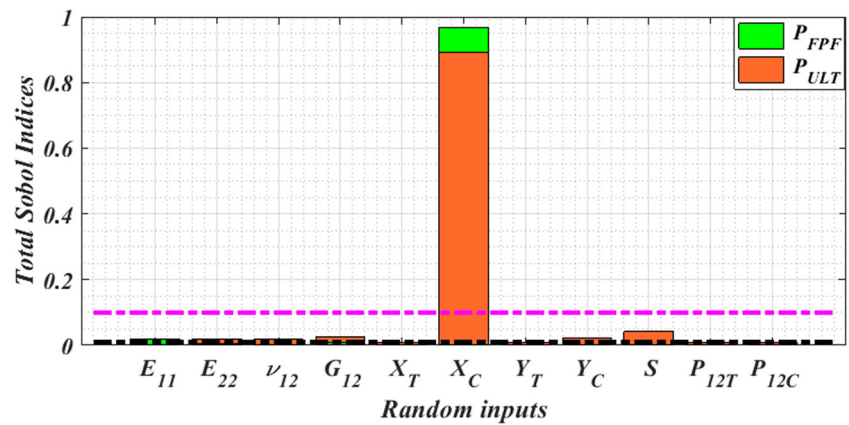


Fig. 16 Damage progression of a composite laminate with circular cut-out subjected to out-of-plane transverse loading (top view or $x-y$ plane of the rotated coordinate system)

Table 5 The statistics for the PFA responses under out-of-plane transverse loading with the stochastic approach

Response			δ_{FPF} (mm)	P_{FPF} (N)	δ_{ULT} (mm)	P_{ULT} (N)
LHS simulation (5000 samples)	Mean		1.6820e+00	3.6197e+02	4.9725e+00	2.8086e+03
	Std		2.4229e-01	8.5382e+01	3.8755e-01	3.1163e+02
PCE	Order =2 (356 samples)	Mean	1.6743e+00	3.5893e+02	4.9744e+00	2.8158e+03
		Std	2.2035e-01	7.5550e+01	3.7547e-01	2.9229e+02
	Order = 3 (928 samples)	Mean	1.6848e+00	3.6271e+02	4.9692e+00	2.8130e+03
		Std	2.4535e-01	8.4281e+01	3.9721e-01	3.1244e+02

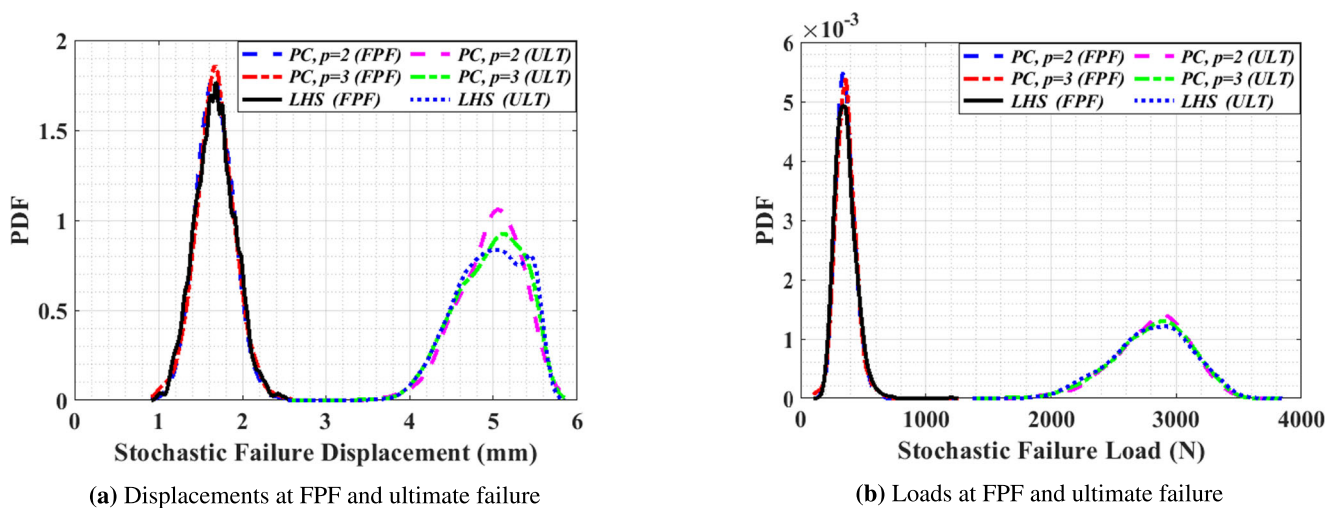


Fig. 17 The PDF plots of the stochastic responses of a composite laminate with a circular cutout subjected to out-of-plane transverse loading

yielding RMSE in the range of 0.1 to 0.5) with some scatter for P_{FPF} in Fig. 18. Nonetheless, the RMSE value for P_{FPF} was around 0.5 only; and hence, the third-order PCE models were accepted. The converged PCE models were then used for GSA by using the same tolerance values for Sobol indices as done in Sections 5.2 and 5.3. In Figs. 19 and 20, a higher number of random inputs are seen to be non-negligible contrarily to that for in-plane tensile and compressive loading cases. For δ_{FPF} and P_{FPF} , the Sobol indices of E_{22} and Y_T have large values than other random

inputs since they influence the matrix failure under tension for FPF significantly. On the other hand, the Sobol indices of E_{11} and X_C are higher than other random inputs for δ_{ULT} and P_{ULT} , which indicates the ultimate failure is mainly dominated by fiber failure under compression.

It is to be noted that the inter-ply delamination (Elder et al. 2008; Thapa et al. 2019a) during out-of-plane deformation was not considered here as the effects of randomness in cohesive parameters on the numerical stability of FEA simulation demand further study. Furthermore, the interlaminar failure analysis generally requires modeling of the plies as solid/continuum shell elements and the cohesive elements of fine mesh size (to avoid mesh sensitivity and convergence issues) in between the plies, which is computationally demanding even for a single FEA simulation. These issues are being tackled by the authors (Thapa et al. 2019a) so that it can be implemented efficiently with the presented framework.

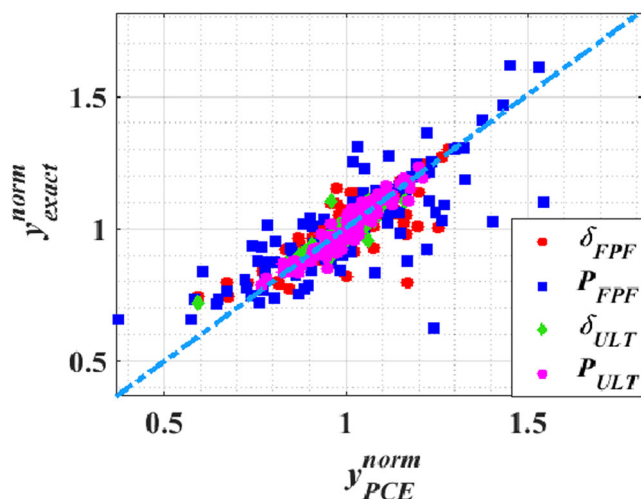
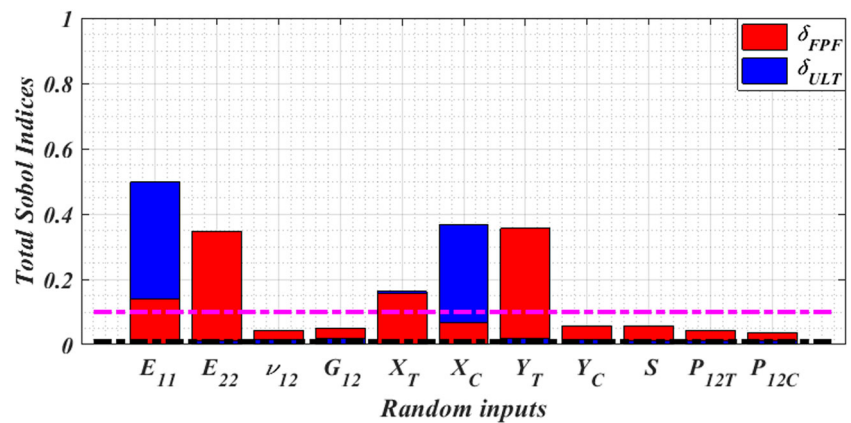


Fig. 18 The normalized cross-validation plot of the stochastic responses with PCE for a composite laminate with a circular cutout subjected to out-of-plane transverse loading. The normalization was carried out by dividing the response values with their corresponding mean values

6 Conclusion

A stochastic framework for UQ and GSA of damage mechanics-material property degradation-based progressive failure responses of composite structures based on a highly accurate and computationally efficient approach called polynomial chaos expansion was presented in this paper. This work was motivated by a limited number of studies related to stochastic PFA using FEA. The main advantage of this approach is that the computationally prohibitive GSA for composites can be carried out with a low number of FEA simulations that are required for the construction of PCE.

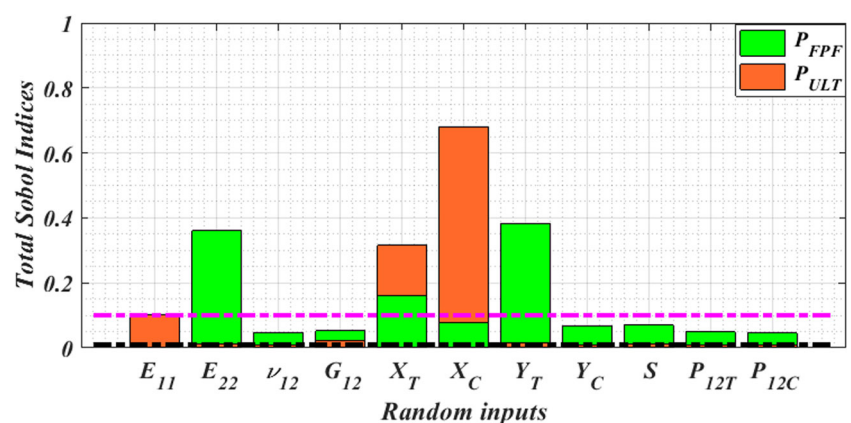
Fig. 19 Total Sobol indices for FPF and ultimate failure displacements of a composite laminate with a circular cutout subjected to out-of-plane transverse loading



To demonstrate the applicability of this approach, a composite laminate with a circular cutout at the center was considered, and the failure responses were studied for three load cases—uniaxial in-plane tension, uniaxial in-plane compression, and out-of-plane transverse loading—under the presence of material uncertainties. Some of the main findings of this study are presented below:

1. The accuracy of the results obtained with the presented framework was similar to that with a large number of LHS simulations in spite of using a substantially low number of samples. This demonstrated the cost-effectiveness of the framework with a similar accuracy to that of the sampling technique.
2. From the GSA using Sobol indices, the contribution of different random input material properties on a particular failure response was found to be unequal. Furthermore, the contributions of random inputs were observed to be response-dependent and demonstrated different patterns for different responses even for the same composite panel.
3. The importance of GSA was underlined by its ability to identify the influential as well as non-influential random input material properties for each failure response. It will be immensely useful in decision making regarding the requirement of further experimental tests for parameter estimation. Also, the non-influential random inputs can be neglected or considered deterministic that will reduce computational effort for further uncertainty analysis or optimization of composites by dimension reduction.
4. The contribution of Puck's parameter on the failure responses was significantly low compared with other influential random inputs such as modulus and strength parameters.
5. The influential random inputs identified by the GSA for failure responses correlated well with the failure modes, thereby demonstrating the capability of the framework to identify failure modes. For instance, for FPF responses in the tensile loading case, the influential random inputs were found to be E_{22} and Y_T , and the failure mode was matrix failure in tension.

Fig. 20 Total Sobol indices for FPF and ultimate failure loads of a composite laminate with a circular cutout subjected to out-of-plane transverse loading



6. The abrupt transition of the failure from FPF to ultimate failure (indicating unstable failure progression) for the in-plane compressive loading case than for tensile and out-of-plane transverse loading cases was more intuitive from the proximity of the location of the PDFs of the failure responses in compressive loading. So, the proximity and overlapping of the FPF and ultimate failure responses can be used to describe the nature of failure progression.
7. The number of FEA simulations/samples required for the presented approach was found to be problem dependent. For instance, for out-of-plane transverse loading, which involved large displacement and high geometric non-linearity, the number of samples required was higher than in tensile and compressive loading.

Hence, the presented approach for stochastic PFA using FEA is a cost-effective approach to understand the effects of uncertainties on the failure responses of composite structures. And, its implementation in the design of composites will be instrumental in obtaining optimal design with enhanced performance behavior and improved reliability. Although the framework was utilized for a composite laminate in this study, it can be easily applied to complex composite structures as well. The future work related to this research includes the implementation of interlaminar failure using cohesive-zone modeling, fracture mechanics-based PFA, consideration of uncertainties in ply thickness/orientation, and application to a composite wing of an aircraft.

Acknowledgments This research was carried out while the first author was on a Graduate Council Fellowship (GCF) during his Ph.D. at the University of Alabama. The authors would like to thank the Research Grants Committee (RGC), Graduate Council Fellowship, the Remote Sensing Center, and the Department of Aerospace Engineering and Mechanics at The University of Alabama, Tuscaloosa for their kind support.

Compliance with ethical standards

Conflict of interest The authors declare that they have no conflict of interest.

Replication of results The MATLAB codes for the presented framework and finite element analysis files for the application problems generated during this study are available in the GitHub repository, <https://github.com/mthapa7/SAMO.UQGSAPFA.CODES.git>.

References

- Ambur DR, Jaunky N, Hilburger M, Davila CG (2004) Progressive failure analyses of compression-loaded composite curved panels with and without cutouts. *Compos Struct* 65(2):143–155
- Camanho P, Maimí P, Dávila C (2007) Prediction of size effects in notched laminates using continuum damage mechanics. *Compos Sci Technol* 67(13):2715–2727
- Chang FK, Chang KY (1987) A progressive damage model for laminated composites containing stress concentrations. *J Compos Mater* 21(9):834–855
- Chang FK, Lessard L, Tang JM (1988) Compression response of laminated composites containing an open hole. *SAMPE Q* (United States) 19(4)
- Chen JF, Morozov EV, Shankar K (2014) Progressive failure analysis of perforated aluminium/CFRP fibre metal laminates using a combined elastoplastic damage model and including delamination effects. *Compos Struct* 114:64–79
- Choi SK, Grandhi R, Canfield RA (2006) Reliability-based structural design. Springer Science & Business Media
- Crestaux T, Le matre O, Martinez JM (2009) Polynomial chaos expansion for sensitivity analysis. *Reliab Eng Syst Saf* 94(7):1161–1172
- Cruz ME, Patera AT (1995) A parallel Monte-Carlo finite-element procedure for the analysis of multicomponent random media. *Int J Numer Methods Eng* 38(7):1087–1121
- Daniel IM (2007) Failure of composite materials. *Strain* 43(1):4–12
- Dey S, Mukhopadhyay T, Adhikari S (2015) Stochastic free vibration analyses of composite shallow doubly curved shells—a kriging model approach. *Compos B Eng* 70:99–112
- Dey S, Mukhopadhyay T, Adhikari S (2017) Metamodel based high-fidelity stochastic analysis of composite laminates: a concise review with critical comparative assessment. *Compos Struct* 171:227–250
- Elder D, Verdaasdonk A, Thomson R (2008) Fastener pull-through in a carbon fibre epoxy composite joint. *Compos Struct* 86(1):291–298. fourteenth International Conference on Composite Structures
- Gadade AM, Lal A, Singh B (2016) Stochastic progressive failure analysis of laminated composite plates using Puck's failure criteria. *Mech Adv Mater Struct* 23(7):739–757
- Garnich MR, Akula VMK (2009) Review of degradation models for progressive failure analysis of fiber reinforced polymer composites. *Appl Mech Rev* 62(1):010801
- Gautschi W (2004) Orthogonal polynomials. Oxford University Press, Oxford
- Ghanem R, Spanos PD (1990) Polynomial chaos in stochastic finite elements
- Günel M, Kayran A (2013) Non-linear progressive failure analysis of open-hole composite laminates under combined loading. *J Sandw Struct Mater* 15(3):309–339
- Hinton MJ, Kaddour AS, Soden PD (2002) A comparison of the predictive capabilities of current failure theories for composite laminates, judged against experimental evidence. *Compos Sci Technol* 62(12-13):1725–1797
- Hinton MJKA, Kaddour AS, Soden PD (2004) Failure criteria in fibre reinforced polymer composites: the world-wide failure exercise. Elsevier
- Hosder S, Walters R, Perez R (2006) A non-intrusive polynomial chaos method for uncertainty propagation in CFD simulations. In: 44th AIAA aerospace sciences meeting and exhibit, p 891
- Hosder S, Walters RW, Balch M (2010) Point-collocation nonintrusive polynomial chaos method for stochastic computational fluid dynamics. *AIAA J* 48(12):2721–2730
- Icardi U, Locatto S, Longo A (2007) Assessment of recent theories for predicting failure of composite laminates. *Appl Mech Rev* 60(2):76–86
- Kamiński M, Kleiber M (2000) Perturbation based stochastic finite element method for homogenization of two-phase elastic composites. *Comput Struct* 78(6):811–826
- Kanouté P, Boso DP, Chaboche JL, Schrefler BA (2009) Multiscale methods for composites: a review. *Arch Comput Methods Eng* 16(1):31–75
- Kleiber M, Hien TD (1992) The stochastic finite element method: basic perturbation technique and computer implementation. Wiley

- Lee CS, Kim JH, Kim SK, Ryu DM, Lee JM (2015) Initial and progressive failure analyses for composite laminates using Puck failure criterion and damage-coupled finite element method. *Compos Struct* 121:406–419
- Li HS, Gu RJ, Zhao X (2017) Global sensitivity analysis of load distribution and displacement in multi-bolt composite joints. *Compos B Eng* 116:200–210
- Liu G, Tay TE, Tan VBC (2010) Failure progression and mesh sensitivity analyses by the plate element-failure method. *J Compos Mater* 44(20):2363–2379
- Liu PF, Zheng J (2008) Progressive failure analysis of carbon fiber/epoxy composite laminates using continuum damage mechanics. *Mater Sci Eng A* 485(1-2):711–717
- Liu WK, Belytschko T, Mani A (1986) Probabilistic finite elements for nonlinear structural dynamics. *Comput Methods Appl Mech Eng* 56:61–81
- Lopes CS, Camanho PP, Gürdal Z, Tatting BF (2007) Progressive failure analysis of tow-placed, variable-stiffness composite panels. *Int J Solids Struct* 44(25-26):8493–8516
- McCartney LN (2005) Energy-based prediction of progressive ply cracking and strength of general symmetric laminates using an homogenisation method. *Compos A: Appl Sci Manuf* 36(2):119–128
- MSC (2007) MSC Nastran 2007 r1, Implicit nonlinear (SOL 600) user's guide. MSC Software
- Murugesan N, Rajamohan V (2017) Prediction of progressive ply failure of laminated composite structures: a review. *Arch Comput Methods Eng* 24(4):841–853
- Navaid MR (2010) Global sensitivity analysis of parameters in Puck's failure theory for laminated composites. PhD thesis, Engineering
- Pal P, Bhattacharyya S (2007) Progressive failure analysis of cross-ply laminated composite plates by finite element method. *J Reinf Plast Compos* 26(5):465–477
- Pal P, Ray C (2002) Progressive failure analysis of laminated composite plates by finite element method. *J Reinf Plast Compos* 21(16):1505–1513
- Puck A, Schürmann H (2004) Failure analysis of FRP laminates by means of physically based phenomenological models. In: *Failure Criteria in Fibre-Reinforced-Polymer Composites*. Elsevier, pp 832–876
- Reddy JN (2003) *Mechanics of laminated composite plates and shells: theory and analysis*. CRC press
- Reddy Y, Moorthy CD, Reddy J (1995) Non-linear progressive failure analysis of laminated composite plates. *Int J Nonlin Mech* 30(5):629–649
- Romanowicz M (2010) Progressive failure analysis of unidirectional fiber-reinforced polymers with inhomogeneous interphase and randomly distributed fibers under transverse tensile loading. *Compos A: Appl Sci Manuf* 41(12):1829–1838
- Sakata S, Ashida F, Kojima T, Zako M (2008a) Influence of uncertainty in microscopic material property on homogenized elastic property of unidirectional fiber reinforced composites. *Theor Appl Mech Japan* 56:67–76
- Sakata S, Ashida F, Zako M (2008b) Stochastic response analysis of FRP using the second-order perturbation-based homogenization method. *J Solid Mech Mater Eng* 2(1):70–81
- Saltelli A, Chan K, Scott M et al (2000) *Sensitivity analysis probability and statistics series*. Wiley, New York
- Sepahvand K (2016) Spectral stochastic finite element vibration analysis of fiber-reinforced composites with random fiber orientation. *Compos Struct* 145:119–128
- Shaw A, Sriramula S, Gosling PD, Chryssanthopoulos MK (2010) A critical reliability evaluation of fibre reinforced composite materials based on probabilistic micro and macro-mechanical analysis. *Compos B Eng* 41(6):446–453
- Sleight DW (1999) Progressive failure analysis methodology for laminated composite structures, NASA/TP-1999-209107. Tech. rep
- Soden PD, Kaddour AS, Hinton MJ (2004) Recommendations for designers and researchers resulting from the world-wide failure exercise. In: *Failure criteria in fibre-reinforced-polymer composites*. Elsevier, pp 1223–1251
- Su Z, Tay T, Ridha M, Chen B (2015) Progressive damage modeling of open-hole composite laminates under compression. *Compos Struct* 122:507–517
- Sudret B (2008) Global sensitivity analysis using polynomial chaos expansions. *Reliab Eng Syst Saf* 93(7):964–979
- Sun X, Tong L, Chen H (2001) Progressive failure analysis of laminated plates with delamination. *J Reinf Plast Compos* 20(16):1370–1389
- Szeg G (1939) *Orthogonal polynomials*, vol 23. American Mathematical Soc
- Tan S, Nuismer R (1989) A theory for progressive matrix cracking in composite laminates. *J Compos Mater* 23(10):1029–1047
- Tan SC, Perez J (1993) Progressive failure of laminated composites with a hole under compressive loading. *J Reinf Plast Compos* 12(10):1043–1057
- Tay TE, Liu G, Tan VBC, Sun XS, Pham DC (2008) Progressive failure analysis of composites. *J Compos Mater* 42(18):1921–1966
- Thapa M, Mulani SB, Walters RW (2018a) A new non-intrusive polynomial chaos using higher order sensitivities. *Comput Methods Appl Mech Eng* 328:594–611
- Thapa M, Mulani SB, Walters RW (2018b) Variance based adaptive-sparse polynomial chaos with adaptive sampling. In: *2018 AIAA Non-deterministic approaches conference*, p 2168
- Thapa M, Jony B, Vishe N, Mulani SB, Roy S (2019a) Comparison of numerical and experimental study of mode-I interlaminar fracture of self-healing composites using cohesive zone modeling. In: *Proceedings of the American Society for Composites—Thirty-fourth Technical Conference*
- Thapa M, Mulani SB, Walters RW (2019b) Stochastic multi-scale modeling of carbon fiber reinforced composites with polynomial chaos. *Compos Struct* 213:82–97
- Thapa M, Mulani SB, Walters RW (2019c) *Uncertainty quantification: advances in research and applications*. Nova
- Thapa M, Mulani SB, Walters RW (2020) Adaptive weighted least-squares polynomial chaos expansion with basis adaptivity and sequential adaptive sampling. *Comput Methods Appl Mech Eng* 360:112759
- Vallmajó O, Cózar I, Furtado C, Tavares R, Arteiro A, Turon A, Camanho P (2019) Virtual calculation of the b-value allowables of notched composite laminates. *Compos Struct* 212:11–21
- Wiener N (1938) The homogeneous chaos. *Am J Math* 60(4):897–936
- Xiu D, Karniadakis GE (2002) The Wiener–Askey polynomial chaos for stochastic differential equations. *SIAM J Sci Comput* 24(2):619–644
- Zhi J, Tay TE (2018) Computational structural analysis of composites with spectral-based stochastic multi-scale method. *Multiscale Model Simul* 1(2):103–118
- Zhou XY, Gosling PD, Pearce CJ, Ullah Z, Kaczmarczyk L (2016) Perturbation-based stochastic multi-scale computational homogenization method for woven textile composites. *Int J Solids Struct* 80:368–380
- Zhu C, Zhu P, Lu J (2018) Global sensitivity analysis for the elastic properties of unidirectional carbon fibre reinforced composites based on metamodels. *Polym Polym Compos* 26(3):205–221

Publisher's note Springer Nature remains neutral with regard to jurisdictional claims in published maps and institutional affiliations.